12-2021

Soil Gypsum Content Analysis of the Proposed Road Route Extension of FM 2185 in the Gypsum Plain, Culberson County, Texas

Chikaodili Ohakawa
Stephen F Austin State University, chikaohakawa@gmail.com

Soil Gypsum Content Analysis of the Proposed Road Route Extension of FM 2185 in the Gypsum Plain, Culberson County, Texas

Creative Commons License

Soil Gypsum Content Analysis of the Proposed Road Route Extension of FM 2185 in the
Gypsum Plain, Culberson County, Texas

By

Chikaodili Ohakawa
Bachelor of Science, Geological Sciences

Presented to the Faculty of the Graduate School of
Stephen F. Austin State University
In Partial Fulfilment
Of the Requirements

For the Degree of
Master of Science in Environmental Science

STEPHEN F. AUSTIN STATE UNIVERSITY
December 2021

Soil Gypsum Content Analysis of the Proposed Road Route Extension of FM 2185 in the Gypsum Plain, Culberson County, Texas

By

Chikaodili Ohakawa

Bachelor of Science, Geological Sciences

APPROVED:

_____
Dr. Kenneth Farrish, Thesis Director

_____
Dr. Kevin Stafford, Committee Member

_____
Dr. I-Kuai Hung, Committee Member

_____
Dr. Julie Bloxson, Committee Member

_____
Freddie Avant, Ph.D.
Interim Dean of Research and Graduate Studies

ABSTRACT

Soils serve as the underlying substrate on which foundations for most structures are built. The properties of a soil type are therefore an important consideration in building engineered structures. Gypsic soils are problematic for construction of such structures. One of the main problems with gypsic soils is dissolution. Gypsum ($CaSO_4 \cdot 2H_2O$) in soils dissolves easily creating voids which can be detrimental to the integrity of engineering structures. To mitigate this, it is important to determine the amount of gypsum present in soils, before construction is initiated.

In this study, three methods were employed in the determination of gypsum content in soils along a proposed road route in the Gypsum Plain, Culberson County, Texas: the wet chemical method, the X-ray fluorescence method and the thermogravimetric method. Results showed no significant difference in gypsum concentrations using the varying methods on samples obtained at the same point in a location, but showed a significant difference in the concentration of samples obtained at different depths in a location. Gypsum contents along the approximately ninety-kilometer road route was predominantly relatively low, with about 65% of sample locations having gypsum content of less than 10%. About 11% of sampling locations, together totaling about three miles of the route, had high gypsum contents of over 70%.

ACKNOWLEDGEMENT

TABLE OF CONTENTS

LIST OF FIGURES

LIST OF TABLES

INTRODUCTION

Gypsum ($CaSO_4 \cdot 2H_2O$) is a highly soluble mineral. Under suitable groundwater flow conditions, rocks and soils rich in gypsum can dissolve and collapse forming caves and karst features. These karst features can exist at the surface, or at various depths beneath the surface, with overlying rock beds. Pressure from the surface or the surrounding beds can lead to collapse of the overlying beds. Also, collapse of caves in the subsurface either by sudden failure of thick overlying beds, or by gradual caving of thinly bedded layers allow for the upward migration of voids, which eventually leads to subsidence of the overlying ground surface (Thompson et al., 1998). This collapse and subsidence in turn impairs the structural integrity of engineering structures at the surface such as buildings, roads, etc.

Farm to Market 2185 (FM 2185) is a planned road route to be constructed in Culberson County, Texas. The planned route exists majorly within the Gypsum Plain of West Texas. Karst features present in the Gypsum Plain of West Texas pose a structural integrity challenge for engineering activities such as road construction, especially when the predominant traffic expected consist of heavy vehicles as those associated with energy sector activities in the region. Pressure from the weight of these vehicles can

cause collapse of the roofs of underlying caves, leading to failure of the roads, and causing possible loss of life and property. To mitigate this, tests need to be carried out to determine gypsum content of the soils and identify locations with high gypsum concentrations present in the soils, as these areas would have a high probability of developing voids in the future. Determining the gypsum contents of the soil will help guide road construction specifications, and where applicable, show the need for alternative road routes by avoiding the most problematic areas.

There are various methods used in determining the amount of gypsum in soils, some of which are slow and expensive, and others requiring complex chemical analytical methods. These methods work well with a small number of samples. However, with larger numbers of samples, a faster and more economic method of sampling is advantageous.

The purpose of this study was to determine soil gypsum concentrations along the planned road route FM 2185, in the Gypsum Plain of Culberson County, Texas. This research evaluated gypsum concentrations in soil samples obtained along the length of the proposed road route FM 2185 using three different methods, and compared the results obtained using the three methods. In addition, a GIS map was produced for the road route which indicates gypsum content of the soils along the proposed route, offering a valuable planning tool.

OBJECTIVES

This research focused on obtaining soil gypsum contents along the proposed FM 2185 road route and on comparing the methods used in the soil gypsum content analysis.

The specific objectives were to:

1. Compare three methods of gypsum analysis- The methods are the wet chemical analysis method, the X-ray fluorescence sampling method and the thermogravimetric (drying) method.

2. Analyze soil samples taken along the proposed FM 2185 route for gypsum content using the methods mentioned above.

3. Construct a GIS map showing soil gypsum content along the proposed road route and identify areas that require further investigation based on the soil gypsum content.

STUDY AREA

The study area was located within the Gypsum Plain in Culberson County, Texas. It is a semi-arid region located in West Texas. Annual precipitation in the region averages 33cm, with the highest rainfall occurring between July-September. Gypsic soils are known to be abundant in the region. Based on engineering classifications, gypsic soils can be classified as either gypsiferous or gypseous soils. Gypsiferous soils are soils that contain gypsum, but the gypsum present does not control the soil properties, while gypseous soils refers to soils in which its properties are controlled by the gypsum present (Herrero et al., 2009). This also means that gypsiferous soils have relatively lower gypsum contents and gypseous soils have a higher gypsum content (Casby-Horton et al., 2015). The soils in the region were found to consist of both gypsiferous and gypseous soils.

The right-of-way for the proposed FM 2185 route was acquired by the State of Texas in the 1960s, but the road was not completed, partly because of concerns about the high gypsum content of the soils along the route. The proposed road will be an extension of the existing rural road FM 2185. Figure 1 shows the location of the existing road and the proposed new road in Culberson County, Texas. The proposed new road will span approximately 48 km, starting at the end of the current pavement of

FM 2185 (Looney Spur Road - 31°25'12.68"N, 104°27'13.70"W) and trending north-east wards to end at the junction with FM 3541 (31°45'28.69"N, 104°13'16.79"W). Activities of companies in the energy sector have been expanding in the area, with hundreds of workers to support drilling activities. According to TxDOT (2020) Statewide Travel Demand Model, traffic on FM 2185 and adjacent roadways is expected to increase from current conditions by up to 300% in the opening year, and truck traffic is expected to account for over 20% of the traffic. The proposed road will aid mobility and access to urgent health care, in case of an emergency.
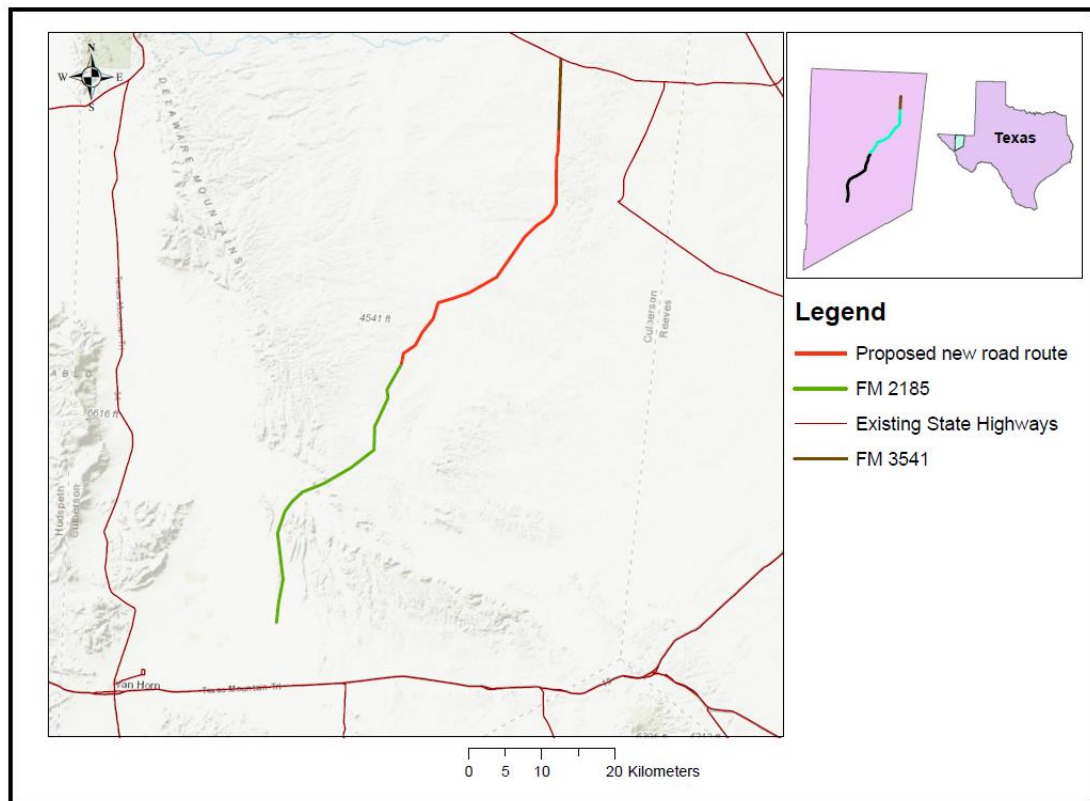
Figure 1: Map showing the existing roads and proposed new road routes in the study area, Culberson County, Texas.

LITERATURE REVIEW

Origin and Geology of the Gypsum Plain

The evaporite karst region of southeastern New Mexico and West Texas is commonly referred to as the Gypsum Plain (Hill, 1996). Spanning an area of about 2800km^2, it is characterized by outcrops of sulfate rocks and associated sulfate-rich soils within the western Delaware Basin (Stafford & Brown, 2019). The Gypsum Plain is one of the greatest accumulations of evaporites in the United States. It is bound to the north by the Guadalupe Mountains, the west by the Delaware Mountains and the south by the Apache Mountains.

Permian strata of the Delaware Basin reach up to 2000m in thickness. Adams et al. (1939) broadly divided the Permian-age Delaware Basin, which constitutes about 95% of the basin (Hill, 1996), into four series: the Wolfcampian Series, Leonardian Series, Guadalupian Series and Ochoan Series.

In Wolfcampian time, the seas spread over the whole of southeastern New Mexico and West Texas. This series is characterized by thick sequences of shale and limestone. In Leonardian time, the seas became progressively restricted so that belts of red beds (consisting of reddish brown to reddish orange siltstone, claystone and fine-grained sandstone) and evaporites encroached farther towards the Delaware Basin. This

series is composed primarily of shale and thin-bedded limestone. By the end of the

Guadalupian, which is composed of massive reef limestone and dolomite, the seas had

become entirely restricted to the Delaware Basin (Hill, 1996; King, 1942). The Ochoan

series, which is characterized by thin red beds and some of the thickest evaporite

deposits in the world, represents the final stages of the Permian seas which had

persisted from the Precambrian times until the Guadalupian (Hill, 1996). These

evaporite deposits marked the closing off and transition of the Delaware Basin from a

marine regime, which had persisted from the Precambrian, to a continental regime.

During Ochoan time, the West Texas/eastern New Mexico area was a continental desert

which was partially sheltered by uplifted ranges with a hot and dry climate to the west

(Hill, 1996). Evaporites are formed from the evaporation of sea water in an enclosed

marine basin (Montgomery, 2000).

The Castile, Salado, Rustler and Dewey Lake formations make up the Ochoan

series, with a thickness of about 1200m-1500m (Hill, 1996). The Castile Formation

consists primarily of anhydrite, the Salado Formation of halite, the Rustler Formation of

dolomite and anhydrite and the Dewey Lake Formation of continental red beds.

Outcrops of the Ochoan series are rarely observed on the surface due to their soluble

nature but can be observed in the subsurface. The Gypsum Plain is made up largely by

the Castile Formation and the Rustler Formation. Figure 2 shows the location of the

Castile Formation within Texas and New Mexico.
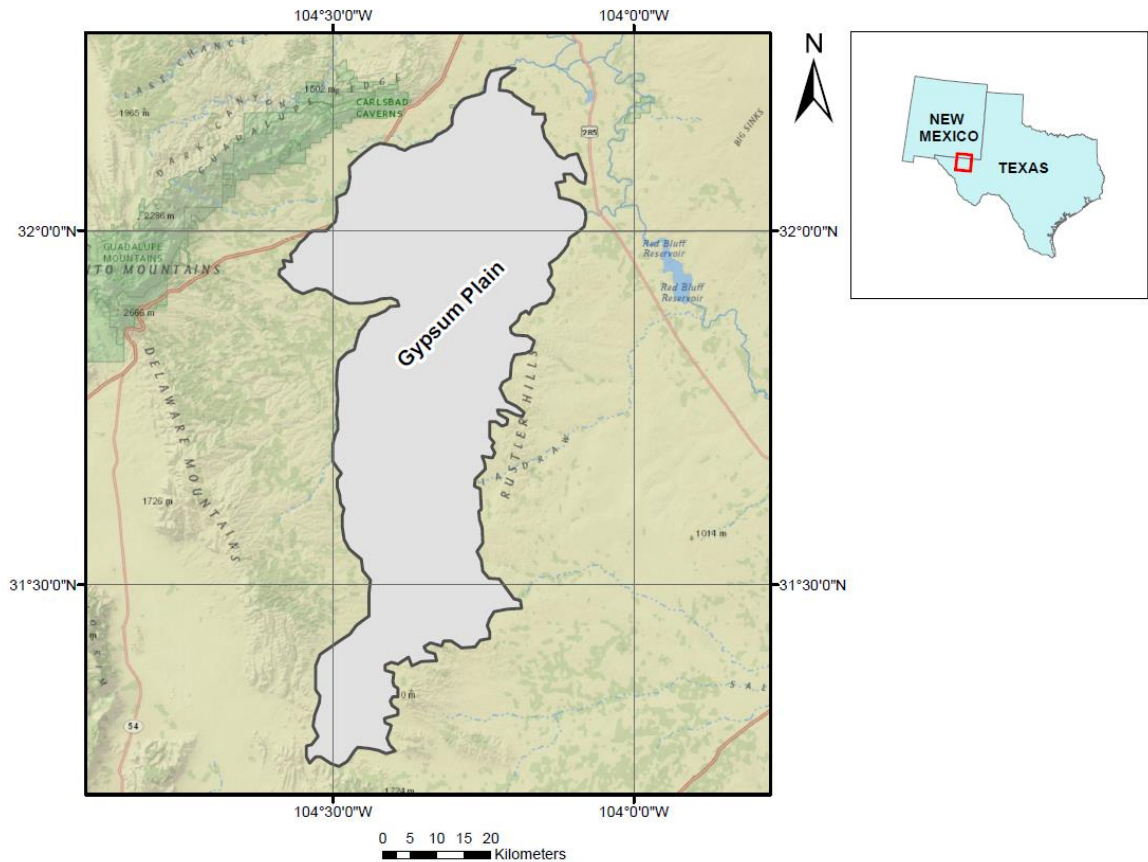
Figure 2: Map showing the Castile Formation of the Gypsum Plain within Texas and New Mexico. (Adapted from Kirkland and Evans 1980).

Castile Formation

The Castile Formation dominates the Gypsum Plain and was deposited in the Delaware Basin at a time marking a transition from marine waters with normal salinity to continental regime (Hill, 1996). The Castile Formation consists of massive to laminated anhydrite (and gypsum) interbedded with halite (Hill, 1996). In the subsurface, it occurs as anhydrite due to burial dehydration. At the surface, anhydrite is hydrated to form gypsum.

The Castile Formation crops out in Eddy County, New Mexico and Culberson County, Texas over an area of approximately 1800km^2 (Stafford, 2013), from the Delaware Mountains on the west to the Rustler Hills on the east, where it dips into the subsurface (Stafford, 2008a). The thickness of the Castile Formation varies based on deposition and dissolution. In the Gypsum Plain area of the Castile Formation, the thickness can range from 0-480m. The greatest thickness of the Castile Formation is found in the southern part of the basin, where it can reach 540m in the subsurface (Hill, 1996). Castile evaporites can be seen at the surface throughout the eastern portion of the Delaware Basin (Stafford et al., 2008a). The Castile Formation is shown below in Figure 3 in relation to surrounding geologic features.

Despite their widespread development, surface outcrops of evaporites are limited because of their low resistance to effects of denudation. Evaporite rocks are highly soluble. Because of this high solubility, a range of karst features can develop rapidly in gypsic soils. The solution kinetics of evaporites encourage development of features like large sinks, incised arroyos and caves that are laterally limited in epigene settings (Stafford et al., 2008b). Karst in gypsum is mainly intrastratal, i.e., developing a range of features in deep-seated settings within the earth's surface. Karst features in gypsum commonly include cavities, caves, sinkholes (dolines), karrens, collapse structures, disappearing streams, springs, etc.
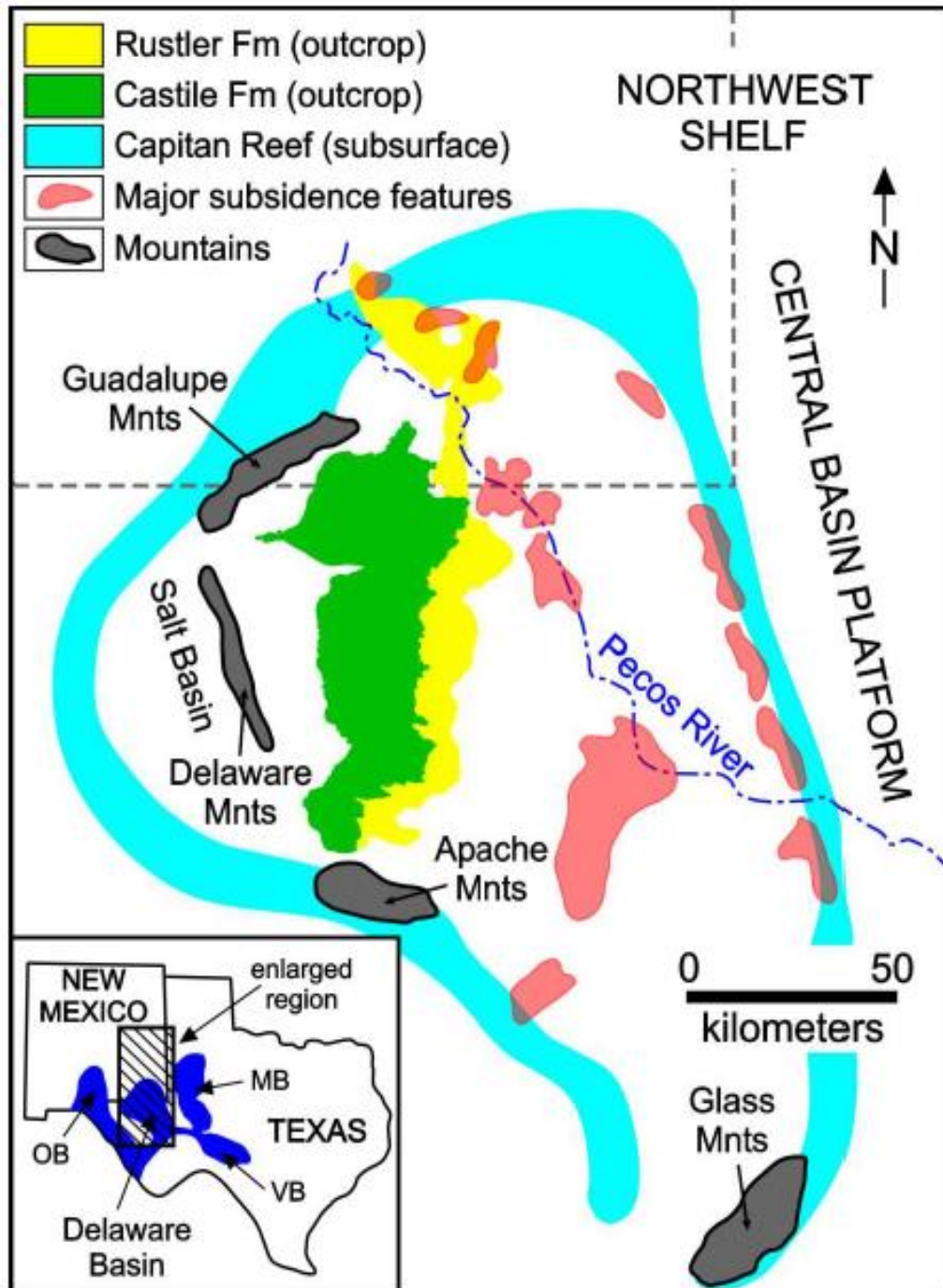
Figure 3: Location of the Castile Formation in relation to surrounding geologic features (after Stafford and Brown, 2019).

The Gypsum Plain comprises abundant sinkholes, caves and closed depressions (Hill, 1996). According to Stafford et al. (2008b), more than 10,000 karst features can be observed on the surface all through the Castile Formation, with surficial karrens, sinkholes and associated caves dominating the landscape. Also, the presence of collapse structures and brecciation signifies subsurface dissolution. They also noted that the distribution of the features is clustered, suggesting hypogenic origins. According to Stafford et al. (2008b), karst features occur in four main forms within the Castile Formation: surficial karst, epigene caves, hypogene caves, and intrastratal brecciation.

Surficial karst within the Castile Formation includes sinkholes, karrens and surficial precipitates. All through the outcrop, sinkholes and closed depressions are abundant, both in open and closed forms (Stafford et al., 2008b). Karren occurs as bare and rocky surfaces that are usually pitted and furrowed. They range in size from as little as 1mm to as large as over 30m (Gunn, 2004). In the Castile, karren occurs extensively in areas of exposed bedrock, which accounts for approximately 8% of the Castile outcrop (Stafford et al., 2008b). Sinkholes are the most dominant karst features present within the Castile. They are formed when water passes over or through a soluble rock, dissolving the material (Gunay, 2002). The sinks created are either by solutional incision of descending waters or collapse of upward stoping subsurface voids. Studies carried out by Stafford et al. (2008b) indicates that sinkholes in the Castile are predominantly collapse features.

Epigene caves within the Castile were found to be well-developed and occurring usually in isolation with concentrations in areas in proximity to a source of descending waters with meteoric origins. These often form large, incised sinkholes connected to small solution conduits, which in turn allows for greater solutional enlargement (Stafford et al., 2008a). These caves are usually small and laterally limited.

Hypogene caves are usually formed by dissolution of soluble rock units by undersaturated fluids ascending from lower formations (Ford & Williams, 2007). Within the Castile, a dense cluster of caves and sinkholes suggest that majority of karst features are of hypogenic origins. These hypogene caves are the longest and deepest observed (Stafford et al., 2008a).

Zones of brecciation are common but varied within the Castile. They are formed from intrastratal dissolution of evaporites, where the void spaces created eventually collapsed (Stafford et al., 2008a). According to (Kirkland & Evans, 1980), brecciation present within the Castile is as a result of dissolution of halite beds which are now almost entirely absent in the Castile outcrop.

Soils in the Castile Formation

Soils cover the earth surface, except in areas having exposed rocks, ice or permafrost, and deep waters. It is also a very important medium for water filtration and waste recycling in nature. Soils have a variety of definitions, the most common being a natural medium for growth of land plants.

The Soil Survey Staff (1999) define soils as a natural body comprising of solids (mineral and/or organic matter), liquids and gases occurring at the land surface, and are characterized by either the ability to support rooted plants in a natural environment or soil horizons, which refers to soil materials that differ from their parent materials as a result of losses, transfers and/or transformation of energy. Soils are broadly divided into organic and mineral soils, based on their constituents. Within the Gypsum Plain, soils present are mineral soils.

Soil profiles contain horizons near the earth surface. These soil horizons have undergone alteration from the original parent material. These alterations can occur as a result of various factors, including climate, relief, living organisms present, etc. The soil horizons are classified into surface and subsurface horizons. Surface soil horizons are referred to as epipedons. Epipedons forms at or near the surface and characteristically display signs of leaching and/or darkening by organic material. Subsurface soil horizons lie beneath the epipedon, but may also be exposed at the surface if there is some sort of truncation.

Certain properties help in classifying soils under a particular horizon. As such, soil horizons are usually diagnostic. Some of these properties include the soil properties, soil materials, soil saturation, soil temperature regimes, soil moisture regimes, soil textural changes, etc.

Soil Temperature Regimes

Soil temperature regimes are used to classify soil series based on the mean annual soil temperature at 10m depth, mean summer temperature; and the difference between mean summer and winter temperatures at a depth of 50cm below the soil surface. According to USDA NRCS, classifications of soil temperature regimes include:

Gelic (Mean annual soil temperature of ≤0°C at a depth of 50cm below soil surface), Cryic (Mean annual soil temperature between 0-8°C, but does not have permafrost), Frigid (Mean annual temperature between 0-8°C), Mesic (Mean annual temperature between 8-15°C), Thermic (Mean annual temperature between 15-22°C) and Hyperthermic (Mean annual temperature of 22°C or higher).

If the difference between the mean summer and mean winter temperatures is less than 6°C, an iso- prefix is included, e.g., isofrigid refers to a regime with mean annual soil temperature between 0-8°C and difference between mean summer and mean winter temperatures ≤ 6°C.

Soil Moisture Regimes

This refers to the presence or absence of groundwater or of water available to keep mesophytic plants alive in the soil or in specific soil horizons during certain periods of the year (USDA NRCS). It is affected by dissolved salts in an area, as water saturated with salts is not available for plants use. There are five classes of soil moisture regime: Aquic soil moisture regime (soils in this regime are saturated with water, but free of

dissolved oxygen), Udic soil moisture regime (soils in this regime are not dry in any part for as long as 90 cumulative days in a year), Xeric soil moisture regime (soils in this regime are moist, in some part, for more than half of the total days per year when the soil temperature at a depth of 50 cm below the soil surface is above 5°C; or for 90 or more consecutive days when the soil temperature at a depth of 50cm is higher than 8°C), Ustic soil moisture regime (soils in this regime have limited moisture, but is such that moisture is present when conditions are suitable for plant growth), and Aridic soil moisture regime (soils in this regime are dry for more than half of the cumulative days in a year where the soil temperature at a depth of 50cm below the soil surface is above 5°C).

Soils in Culberson County, which largely hosts the Gypsum Plain are mostly in the Aridic soil moisture regime (USDA NRCS, 1999). Soils with Aridic soil moisture regime normally occur in areas with arid or semi-arid climate. There is little or no leaching in this soil moisture regime and soluble salts accumulate in the soils if there is a source.

Soil Orders

Based on soil horizons present, soils around the world are classified into twelve soil orders. A soil order can have one or more surface or subsurface horizon present. Soil orders include Gelisols, Histosols, Spodosols, Andisols, Oxisols, Vertisols, Aridisols, Ultisols, Mollisols, Alfisols, Inceptisols, and Entisols. Within Texas, seven of these soil orders are dominant. Figure 4 shows these dominant soil orders in Texas.
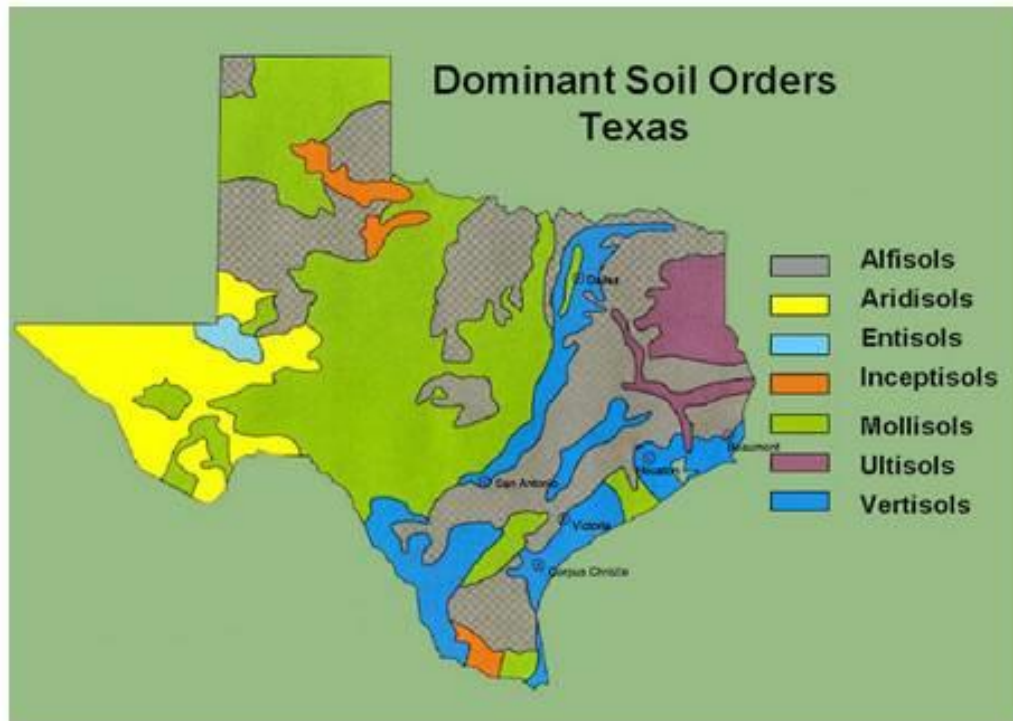
Figure 4: Map showing the dominant soil orders within Texas (From USDA NRCS)

The dominant soil order in Culberson County, in which the Castile Formation lies, are the Aridisols, with Entisols and Mollisols occurring in very few areas. Aridisols generally refers to soil types that have moisture for less than 90 days in a year. Soils in Culberson County falls within the thermic soil temperature regime (15°C to <22°C), and aridic or ustic soil moisture regimes. Two of the main factors that affect soil formation in arid and semi-arid areas are daily temperature variations and lack of water (Verheye, 2009). Soil pedogenic processes are controlled by the moisture regime, and to a lesser extent the temperature regime in a given area (USDA, 1999). Aridisols occupy 12.7% of the total ice-free land globally, and occupy about 9% of land in the United States.

Generally characterized by dry soils and occurring mostly level to hilly lands and depression areas, they are typically saline or alkaline in nature, with very little organic matter present; and have very sparse vegetation made up mainly of xerophytic shrubs and grasses with typically short life cycles. Aridisols are commonly characterized by an Ochric or Anthropic epipedons. They accumulate materials that are easily leached from soils in humid environments, such as calcium carbonate, gypsum, salt, etc. Aridisols are divided into seven suborders, each of which are further divided into great-groups and groups. The seven suborders are: Cryids (Aridisols in cold areas), Salids (Aridisols with accumulation of salts more soluble than gypsum), Durids (Aridisols with accumulation of silica), Gypsids (Aridisols with accumulation of gypsum), Argids (Aridisols with accumulation of clay), Calcids (Aridisols with an accumulation of carbonates), and Cambids (other Aridisols that has undergone transport and change of parent material). Aridisols occur in the Gypsum Plain as either Gypsic soils (soils with accumulated gypsum), Calcic soils (soils with accumulated carbonates), or Cambic soils (soils with pedogenic change, but limited illuviated material) (USDA, 2013). Gypsic soils occur largely within the Gypsum Plain, with soil textures ranging from fine and gravelly loam to fine sand.

Gypsids

Gypsids are the Aridisols that have a gypsic or petrogypsic horizon within 100cm of the soil surface. A gypsic horizon represents a soil horizon in which gypsum has been

accumulated or transformed to a significant extent. A soil horizon is considered Gypsic if it has a thickness of 15cm or more, consists of gypsum greater than 5% weight, has more than 1% visible secondary gypsum that has been transformed or accumulated, and is not cemented by gypsum, with or without other cementing agents. A petrogypsic horizon is one in which visible secondary gypsum has been transformed or accumulated. A soil horizon is considered petrogypsic if it has a thickness of 5mm or more, has gypsum greater than 40% by weight, is cemented by gypsum, with or without other cementing agents, and has lateral continuity. Gypsic and Petrogypsic horizons typically occur as a subsurface horizon, although in some cases, they may also occur at the surface. Gypsids present a major constraint to soil use. The dissolution of gypsum, which is the major constraint, can cause damage to engineering structures.

Formation of Gypsic and Petrogypsic Soils

Soils with a petrogypsic horizon comprise about 30km^2, while soils with a gypsic horizon comprise 9,062km^2 of the conterminous United States (USDA-NRCS, 1997). The key factors in the formation of soils with gypsic horizons are the parent materials, climate and relief (USDA-NRCS, 1997). In most of the areas having gypsum-rich soil, there exists underlying bedrock, rich in gypsum (Bockheim, 2014). Gypsic horizons forms typically in areas with slope between 2 to 16%, aridic soil moisture regime, mesic or thermic soil temperature regime.

Other pedogenic processes that affect the formation of gypsic horizon include calcification, argilluviation, solonization, salinization, and gypsiturbation (Bockheim, 2014).

Soils with gypsic or petrogypsic horizons usually contain an ochric epipedon, with other subsurface horizons present. Subsurface horizons that occur with soils with a gypsic horizon include calcic (referred to as calcigypsids), argillic (argigypsids), natric (natrigypsids), cambic and salic horizons (haplogypsids). Table 1 shows a breakdown of soil types with gypsids.

Table 1: Soil Taxonomy classification of soils with gypsids.

Order	Suborder	Great Group	Subgroups
Aridisols	Gypsids	Argigypsids	Typic, Lithic, Vertic, Calcic, Petronodic, Vitrixerandic, Vitrandic, Xeric, Ustic
		Calcigypsids	Typic, Lithic, Petronodic, Ustic, Vitrandic, Vitrixerandic, Xeric
		Haplogypsids	Typic, Lithic, Leptic, Sodic, Petronodic, Vitrixerandic, Vitrandic, Xeric, Ustic
		Natrigypsids	Typic, Lithic, Vertic, Petronodic, Vitrixerandic, Vitrandic, Xeric, Ustic
		Petrogypsids	Typic, Petrocalcic, Calcic, Vitrixerandic, Vitrandic, Xeric, Ustic

Soil Series within the Castile Formation

USDA differentiates soils into soils map units using areas that indicate a dominant type of soil. A map of the soil map units associated with the Castile Formation is shown in Figure 5. Within the Gypsum Plain, the following map units are mapped:

Beach soils, which are shallow, well-drained, moderately permeable soils formed from fine-grained metamorphic sandstone parent material. They are thermic lithic, Ustic Torriorthents, with slopes ranging from 1 to 70%.

Chilicotal soils are very well-drained loamy-gravelly soils formed in sediments from igneous mountain parent materials. They are thermic, Ustic-Haplocalcids, with slopes ranging from 1 to 50%.

Bissett soils are shallow, well-drained soils formed from weathered limestone parent materials. They are thermic lithic Ustic Haplocalcids, typically consisting of gravelly loam, with slopes ranging from 1 to 70%.

Chispa soils are deep, well-drained, moderately permeable soils, formed in loamy sediment parent materials of various origins. They are thermic Ustic Haplocalcids, consisting of fine-loamy soils, with slopes ranging from 1 to 15%.

Tenneco soils are deep, well-drained soils, formed in deep alluvium. They occur on flood plains, with slopes ranging from 0-5%. They are thermic Ustic Haplocambids, characterized by fine sandy-loam texture.

Culberspeth soils are shallow, well-drained soils, formed in alluvium from predominantly limestone parent materials. They occur on alluvial fans, with slopes ranging from 1-8%. They are thermic, shallow, Calcic Petrocalcids, characterized by gravelly loam.

Dellahunt soils are very deep, well-drained soils, formed in alluvium from sandstone and rock gypsum parent materials. They occur on alluvial fans, alluvial flats and inset fans in karst, with slopes ranging from 0-5%. They are thermic, Ustic Calcigypsids, characterized by loamy textures.

Joberanch soils are shallow, well-drained soils, formed in alluvium from sandstone and rock gypsum parent materials. They occur on alluvial flats, with slopes ranging from 1-3%. They are thermic, shallow, Ustic Petrogypsids, characterized by loam textures.

Neimahr soils are very shallow, well-drained soils, formed in alluvium from sandstone and rock gypsum parent materials. They occur on alluvial flats, with slopes ranging from 1-3%. They are thermic, lithic, Ustic Haplocambids, characterized by fine sandy-loam.

Elcor soils are very shallow, well-drained soils, formed in gypseous residuum parent materials weathered from the Castile Formation. They occur on hills and side slopes in karst, with slopes ranging from 0 to 30%. They are thermic, lithic, Haplogypsids, characterized by gypsiferous-loam textures.

Pokorny soils are very shallow, well-drained soils, formed in alluvium from rock gypsum parent materials from the Castile and Salado formations. They occur on alluvial flats and low hills, with slopes ranging from 0-8%. They are thermic, shallow, Ustic Petrogypsids, characterized by fine-gypseous, hypergypsic loam textures.

Monahans soils consists of very-deep, well-drained, moderately permeable soils, formed in ancient alluvium with significant amounts of gypsum and calcium carbonate parent materials. They occur on upland plains, with slopes ranging from 0-5%. They are thermic, Typic Calcigypsids, characterized by coarse-loamy and fine sandy-loam textures.

Reyab soils consists of very-deep, well-drained, moderately slowly permeable soils, formed in alluvium derived from limestone parent materials. They occur on flood plains, alluvial bottoms and inset fans, with slopes ranging from 0-5%. They are thermic, Ustic Haplocambids, characterized by fine-silty loam textures.

Walkerwells soils consists of very-deep, well-drained soils, formed in alluvium derived from sandstone parent material. They occur on flood plains and drainageways in karst, with slopes ranging from 0-3%. They are thermic, Ustifluventic Haplocambids, characterized by fine-silty clay loam textures.

Hollebeke soils consists of very shallow, well-drained soils with slow runoff and moderate permeability, formed in gypseous residuum parent materials weathered from the Castile Formation with alluvium of silicate material. They occur on low hills in karst,

with slopes ranging from 1-8%. They are thermic, shallow, Ustic Petrogypsids,

characterized by fine-gypseous, hypergypsic loam textures.
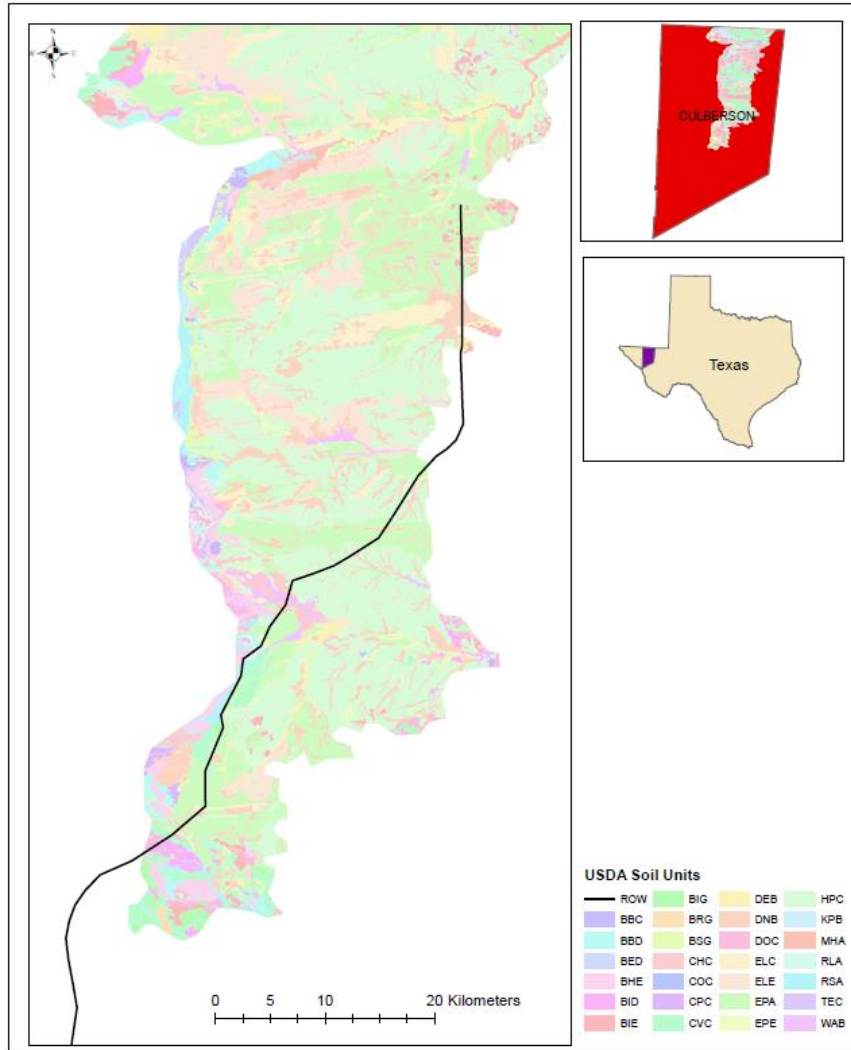
Figure 5: Soil map of the Castile Formation-Gypsum Plain within Texas showing soil map units: BBC, BBD (Beach Sandy-Loam); BED(Beach-Tenneco Complex); BHE (Bissett-Beach complex); BID,BIE,BIG,BRG,BSG(Bissett-Rock outcrop Complex); CHC(Chilicotal Loam); COC(Chispa-Chilicotal Complex); CPC(Chispa Tenneco Complex); CVC(Chispa-Culberspeth Complex); DEB(Dellahunt Silt Loam); DNB(Dellahunt-Neimahr-Joberanch Complex); DOC(Double Loam); ELC,ELE(Elcor Fine Gypsum); APA(Elcor-Dellahunt-Pokorny Complex); EPE(Elcor-Pokorny-Hollomex-Waterwells complex); HPC(Hollebeke-Pokorny Complex); KPB(Kinco-Aguena-Perilla Complex); MHA(Monahans Sandy Loam); RLA(Reyab Loam; RSA(Reyab Silt-Loam); TEC(Tenneco Silt-Loam); WAB(Walkerwells Clay Loam) (After Culberson County Soil Survey, USDA 2013).

The predominant soil map unit within the Gypsum Plain in Texas is the Hollebeke-Pokorny Complex (HPC), having slopes of 1-8%, closely followed by the Elcor-Dellahunt-Pokorny (EPA) Complex, having 0-2% slopes, the Dellahunt-Neimahr-Joberanch (DNB) complex with 1-3% slopes and the Elcor fine-gypsum material (ELE), with 5-30% slopes. These four soil complexes make up approximately 75% of the Gypsum Plain within Texas. Various combinations of the other soil types mentioned above make up the remaining 25%.

Physiography of the Gypsum Plain

Gypsum is readily soluble in water. It is much more soluble than limestone, with solubility ($2.53gL^{-1}$) up to three orders of magnitude greater than limestone in pure water (Gunn, 2004; Stafford et al., 2008b). This high solubility gives rise to widespread development of karst features in evaporites more readily than in limestone. Halite (NaCl) is however much more soluble than gypsum, with its solubility up to 140 times that of gypsum (Gunn, 2004).

Karst features in gypsum are formed either by solution or collapse of the surrounding and overlying rocks (Stafford, 2008a). According to Johnson (1996), there are four basic requirements for the development of gypsum karst: gypsum deposit, water unsaturated with $CaSO_4$, an outlet for the resulting gypsiferous water to escape through, and energy to cause the water to flow.

The Gypsum Plain is in a semi-arid environment, with an annual average precipitation of about 33cm, and the highest precipitation events occurring between July to September. Annual temperature averages 17.3°C with an average annual minimum and maximum of 9.2°C and 25.2°C, respectively (Stafford, 2008a), classifying it under the thermic soil temperature regime and aridic soil moisture regime.

Because of this low precipitation, the Gypsum Plain has maintained extensive outcrops of evaporitic rocks. According to Stafford (2013), water resources in the Castile outcrop are scarce and limited to occasional springs, seeps and caves that breach phreatic conduits. This does not, however, mean an absence of karst features in the area. Stafford (2013) noted the presence of unique evaporite-karst development including extensive caves and rapidly evolving landscape, despite the complex and poorly understood hydrogeologic system of the Castile Formation.

Therefore, to understand karst features and their formations in an area with gypsic soils, the drainage of the area must be understood. The drainage in an area is a function of the climatic and hydrologic conditions of that area (i.e., groundwater flow systems, precipitation events, etc.). Formation of gypsic horizons are typically associated with playa basins, where leaching is limited by a high water table, and eolian salts are recycled from the playa to the surrounding basins (Buol et al., 2011). Stafford (2013) noted that there are abundant fluctuations in fluid chemistry and water table levels over large distances across the Gypsum Plain. Studies carried out by Morris (2018) sought to

understand the dissolution rates of soil materials in the Gypsum Plain. He observed that infiltration was moderate to high in the thick and heterogenous soil complexes, but low in the thin, fine soils. The soil complexes within the Gypsum Plain are mostly fine soils, hence there is a generally low rate of infiltration within the Gypsum Plain.

According to Stafford et al., (2008a), most springs and seeps within the Castile Formation, which hosts the Gypsum Plain, have high amounts of total dissolved solids, primarily sulfate, due to saturation when passing through gypsum-rich facies. Because of the high solubility of evaporites, rapid dissolution occurs at the surfaces, through epigenic processes, forming sinkholes, caves, and incised arroyos, which are laterally extensive and decreases away from the recharge inflows (Stafford et al., 2008a). Also, forced and free convection, established by regional hydraulic gradients in confined settings and steep density gradients in fresh water, respectively, serves to dissolve evaporites through hypogenic processes by sinking of saturated fluids and upward movement of unsaturated fluids, based on density differences (Stafford et al., 2008a).

Engineering Problems Associated with Gypsic Soils

Gypsum ($CaSO_4 \cdot 2H_2O$) is a sulfate mineral usually naturally occurring alongside anhydrite ($CaSO_4$), calcite ($CaCO_3$) or halite ($NaCl$). It is the most common sulfate mineral, and is highly soluble, being about 150 times more soluble than limestone (Gunay, 2002). Dissolution of gypsum may give rise to voids and cavities in the subsurface. According to Yilmaz (2001), karst features in gypsum can be found

throughout the rock mass, either as voids resulting from solution weathering at the surface or along discontinuities, or as cave systems at depths related to present or past groundwater levels. The primary hazard associated with these features is subsidence (Yilmaz, 2007). Karst features may include sinkholes, caves, natural bridges, disappearing streams and springs. These karst features are potentially serious hazards, posing a problem to development of infrastructure in areas they are found. Human activities can serve to induce or further the process of karst formation in areas with gypsum rocks. Some of these activities include:

Reservoir and Dam Construction

Enhanced water flow, due to the constructed structures, and the associated higher dissolution rate, can reactivate the karst system (Yaoru & Cooper, 1997) by raising the water table in previously unsaturated gypsum rocks in the surrounding areas. Dams and reservoirs built on gypsum karst are prone to leakage through the karst conduits, and may ultimately result in collapse of the structure. The underlying cause of dam collapse is usually a lack of understanding of the full scale of the gypsum rocks and its cavities beneath the foundation (Cooper & Guiterrez, 2013). The construction of dams or reservoirs increase the hydraulic gradient and raises the water table, both of which can lead to increased dissolution if gypsum rocks occur at the foundation (Klimchouk & Andrejchuk, 1996). Many dam failures associated with gypsum have occurred around the world. The most infamous of them is the collapse of St Francis dam

in California, USA in 1928, which claimed over 400 lives and millions of dollars

(Klimchouk & Andrejchuk, 1996). Failure was attributed to dissolution of gypsum veins

beneath the dam foundations (Cooper & Guiterrez, 2013).

Mining/Petroleum Industry Activities

Dissolution cavities can be introduced, usually unintentionally, by drilling. Water

from surrounding aquifers can enter a borehole, causing dissolution and forming

cavities which migrate upwards over time. The cavity may expand and become too

large, causing the roof to collapse. This can result in land subsidence or catastrophic

collapse, and the creation of sinkholes more than 10m wide and tens of meters deep

(Johnson, 2008). Mining for materials in layers that overlie or underlie gypsum deposits

can activate the karst processes in the gypsum. Phreatic conduits filled with water can

trigger a rush-in of water and cause mine-flooding (Cooper & Guiterrez, 2013). This type

of underground flooding can cause the development of sinkholes and disruption of

surface drainage. Also, extraction of materials found associated with gypsum, such as

salts, by underground leaching method can induce subsidence processes and collapse in

the overlying layers, thereby increasing karst development (Klimchouk & Andrejchuk,

1996).

Water Abstraction

Abstraction of groundwater from gypsum karst aquifers highly impacts the

development of karst in gypsum. Water abstraction may lower the water table and

cause sediments to be deposited in the gypsum karst. This can in turn cause collapse of the cover deposits resulting in subsidence (Cooper, 2002).

To mitigate these potential hazards, there exists a need to investigate areas prone to formation of karst features, especially where gypsum is known to be present in the bedrock, prior to construction of infrastructure. Sinkholes and other karst features are traditionally investigated using geological and geophysical methods.

Gypsic Soil Sampling

While geologic and geophysical methods can be used in sampling for voids and sinkholes in situ, there is a need to qualify and quantify the mineral composition of the soils present. Gypsum can be identified in the field by morphologic investigation or a simple chemical test. Gypsum appears as yellowish-white, sugar-sized grains under a magnifying glass. The chemical test involves shaking a sample of the soil with water in a test tube and adding a few drops of $BaCl_2$. The development of turbidity signals the presence of gypsum (Porta, 1998).

In planning for construction of structures such as roads in areas where gypsum is known to occur, it is necessary to have an accurate measure of the amount, and possibly concentration of gypsum present. Areas that are wholly gypsum can be dissolved entirely in a quicker amount of time, compared to places that have gypsum occurring with other less soluble rock types. These areas, when identified, can be reinforced, or

offset prior to construction. Researchers have put forward various methods to quantify gypsum content in soils. Some of these include:

Wet Chemical Analysis

Several analytical methods fall under this category, with most using methods based on sulfate (SO_4) determination. These methods are usually slow, require complex chemical analysis, and are often expensive. The main basis for the wet chemical analysis is the separate determination of sulfate and calcium ions (Herrero et al., 2016). In using wet chemical analysis method, complete dissolution of all the gypsum in the given sample must occur; therefore, due to the rate of solubility of gypsum in water ($2.6gL^{-1}$ at 25°C), a low soil to water ratio is required (Porta, 1998). According to Nelson (1982), as the fineness of gypsum crystals increases, its dissolution rate in water also increases, meaning larger gypsum crystals take longer to dissolve compared to smaller crystals. Therefore, the soil to water ratio must be low and enough time must be allowed for the gypsum to be completely dissolved. Sulfate in the samples may be from other sources besides gypsum, hence the possibility of inaccuracies.

Using chemical analysis to obtain the exact amount of gypsum in soils is somewhat difficult. A common method of wet chemical analysis of gypsum concentration involves using acetone as a reagent. The dissolved gypsum is partly precipitated using acetone, and the precipitate re-dissolved in water (Porta, 1998). The gypsum is then determined by measuring the Ca^{2+} in solution.

Limitations to this method using acetone include the dissolution of calcium or

sulfates from other sources, such as carbonates, present in the sample alongside

gypsum. This results in obtaining a higher concentration of calcium and sulfate ions, and

wrongfully classifying it as though it were wholly from the gypsum (USDA Agriculture

Handbook No. 60, 1954). Another method is dissolution in concentrated hydrochloric

acid and precipitation with Ba^{2+}. Sulfate content from the resulting barium sulfate is

determined by gravimetry. This method is, however, long and tedious and will also

report sulfate contents from other sources.

According to Herrero et al. (2016), wet chemical analysis methods are not

appropriate for most soils or gypsum-rich materials. They work well in measuring the

individual components of gypsum (i.e., the calcium and sulfate concentrations), but not

the gypsum concentration itself. Lagerwerff et al. (1965) also stated that corrections

may be necessary for exchange errors. Using these methods, therefore, is not feasible

when it comes to testing for gypsum in soils over a large area, due to the timing

involved, potential for errors and high costs.

X-Ray Methods

X-ray diffraction (XRD) can be used to determine gypsum concentrations. It is a

non-destructive analytical method that can qualify and quantify minerals in a sample,

and can also be used to analyze phase composition and structure. XRD works by

irradiating a material with incident X-rays and then measuring the resulting intensities

and scattering angles of the X-rays that leave the material. However, according to Herrero et al. (2009), this method produces only semi-reliable data for samples that contain 50% gypsum or less, and is not suitable for quantifying gypsum contents in samples with over 50% gypsum. This makes it an unsuitable method for quantifying gypsum in high concentrations.

X-ray fluorescence (XRF) analysis is another way to quantify the gypsum contents of a soil sample. It is widely used to quantify elements in geological and environmental studies (Weindorf et al., 2009). It works by measuring the secondary x-ray emitted from a sample when it is excited by a primary x-ray source. X-ray fluorescence can be used to classify a wide range of elements, including calcium and sulfur in soils, and it provides non-destructive elemental analysis of alloy materials, metals and even trace elements. Experiments using XRF shows that it can detect concentrations ranging from very low concentrations of trace metals to very high concentrations of SiO_2. X-ray fluorescence analysis can be done using a portable XRF analyzer, which directs a radiation beam on the sample for a set amount of time. Kalnicky & Singhvi (2001) noted that elements present in a sample at higher concentrations have a higher detection limit compared to those with lower concentrations. They also noted that with increased sampling times, the method detection limit decreases.

Thermogravimetry

Thermogravimetry is based on weight loss as a result of dehydration, which occurs when a sample containing gypsum undergoes heating. This method serves as a base method which other researchers refined for measuring gypsum. Methods involving drying of the water contents of samples were put forward by Nelson et al. (1978) and Viellefon (1979).

The thermogravimetric properties of gypsum have been widely used in gypsum content determination and thermobalances are often used for accurate measurements (Artieda, 2006; Karanthanasis, 2008). A thermobalance has a maximum load of 1g and a sensitivity of 1µg, and requires conditions, such as gas purging, to work effectively. Therefore, it can only be used for small sample sizes and is not an ideal method for analyzing gypsum for environmental applications as it will most likely not be representative of the actual gypsum contents in soil samples (Karanthanasis, 2008).

Gypsum ($CaSO_4 \cdot 2H_2O$) has two water molecules bound in it, which can be released by heating at a specific temperature. The heating of gypsum, which is a difficult-to-reverse process that destroys gypsum, converts it initially into bassanite ($CaSO_4 \cdot \frac{1}{2}H_2O$) and then anhydrite ($CaSO_4$) (Herrero et al., 2016).

Natural gypsum may contain both free water and bound water. Free water, as the name implies, is not chemically held to the gypsum molecule. It is usually a result of the soil moisture content, and can be removed by drying at relatively low temperatures.

Studies have been carried out to determine this temperature limit. Hill (1937) described

works from previous authors who set this temperature at values ranging from 37.5°C to

as high as 63.5°C, but none of the tests by these authors carried complete conviction.

Conclusive tests carried out by Hill (1937) puts this temperature at 42°C. Herrero et al.

(2016) and Porta (1998) suggests that samples be dried at room temperature, and if

using an oven, temperatures should not exceed 40°C.

The two molecules of water present in gypsum ($CaSO_4 \cdot 2H_2O$) is referred to as

bound water. Bound water is bound to the gypsum molecule and can be removed at

higher temperatures, thereby converting gypsum to anhydrite. According to Porta

(1998), gypsum is totally converted to anhydrite at about 200°C. Using the molecular

weights of gypsum and that of water, the percentage of gypsum present can be

estimated. Water makes up 20.92% of the weight of gypsum. The concentration of

gypsum in this method is also interpolated using the molecular weight of water.

MATERIALS AND METHODS

Field Sample Collection

Samples were previously collected along the length of the existing paved portion of FM 2185 and the proposed road extension, at 400 meter intervals. For each sampling location, samples were collected from both the surface and the subsurface at a depth of about 10cm, and the respective sample locations recorded. There was a total of 242 marked sampling locations with a total of 481 samples collected, three sample locations were on exposed bedrock and thus limited to surface samples. Samples collected included gypseous and gypsiferous type. Samples were collected and sealed in plastic bags. Sample collection was done in the summer of 2019.

Sample Preparation

All samples were crushed and passed through a 2mm sieve to remove coarse fragments and any plant parts in them. They were then dried at 40°C to constant weight, to remove free water content. All further analyses were carried out using the dried samples. Samples were tested to determine the concentration of gypsum in each sample using the XRF analysis and thermogravimetric methods. Randomly selected samples, ten from the surface and ten from the subsurface were also tested using the

wet chemical analysis method to determine gypsum concentration. Reagent grade gypsum and silica, with at least 99% purity, was purchased from a chemical supply company to serve as a standard with which to determine temperature limits and to determine accuracy.

Laboratory Analysis

Wet Chemical Analysis

Twenty samples were selected randomly to undergo chemical analysis. Ten locations were randomly selected, and surface and subsurface samples taken from each of these locations to make up the twenty samples. The analyses were carried out by a commercial laboratory (Analab, Kilgore, Texas) which is NELAC certified. EPA methods 3050B and 9056 were used in preparing the samples for analysis. EPA method 9056, which is the determination of inorganic anions by ion chromatography was used to determine the water extractable sulfate contents of the samples. EPA method 6010C which is inductively coupled plasma-atomic emission spectroscopy (ICP-AES) was used to determine the sulfur and calcium concentrations in milligrams per kilogram (mg/kg) and was then converted to grams per kilogram (g/kg). All computations were done by the laboratory. Sulfur content of the water- soluble sulfate was calculated using the formula below:

$$\frac{32.06}{96.06} * \text{Water-Extractable Sulfate}$$

Where 32.06 is the molecular weight of sulfur and 96.06 is the molecular weight of

sulfate. The value obtained was then subtracted from the sulfur concentration to obtain

a corrected sulfur value.

The final gypsum concentration was calculated using the corrected sulfur value

with the formula:

$$5.37* \text{ Corrected sulfur value}$$

where 5.37 represents the ratio of the molecular weights of gypsum to sulfur.

This method of sampling is expensive, hence the small number of samples tested

via this means.

X-Ray Fluorescence

A battery-powered Niton XL 3t GOLDD+ portable XRF Analyzer by Thermo Fisher

Scientific was used for this analysis. The XRF works by measuring the secondary x-ray

emitted from a sample when it is excited by a primary x-ray source. Each element

produces x-rays with different energy levels and abundance. The detector then

captures, counts and identifies the various energy levels emitted. It is then processed to

reflect concentration estimates for each element.

Samples to be tested were packed into a 32mm double open ended XRF sample

cup and capped with a thin polypropylene film. The XRF analyzer was standardized using

the NIST 2709a PP 180-649 quartz standard associated with the analyzer. The sample

cups were then fitted tightly over the aperture, where an x-ray beam is directed through

the thin film to the sample. Measurements were made using the soils mode, for a total

exposure time of 180secs per sample. Measurements for calcium and sulfur were made

in parts per million (ppm) and converted to grams per kg (g/kg) for easier display. The

data obtained was then exported from the XRF to MS Excel for further processing and

statistical analysis.

Thermogravimetric Analysis

Initial tests were carried out to determine temperature limits. This was done

using the reagent-grade sample of gypsum (with a known concentration), and two field

samples, one with a high gypsum content, and the other with a low gypsum content

(low and high contents estimated visually). A beaker was weighed empty and samples

were added to the beaker and weighed. The samples were heated in the oven starting

from 30°C and reweighed. All masses were recorded to the nearest 0.01g. Temperatures

were increased by 10°C increments up until 200°C. After heating at each temperature,

the samples were cooled in a desiccator. The samples were then weighed and the

process repeated until no further changes in weight were observed. The moisture loss

was then calculated and subsequently the gypsum content. The established

temperature limits served as the temperature basis for sample analysis. Gypsum

contains two water molecules, corresponding to 20.93% of a gypsum molecule.

The reagent grade gypsum did not contain any moisture (free water). The first

observed weight change was between 70°C and 80°C where the sample was found to

have lost three-quarters of its water content. Hence, we concluded that a gypsum sample is converted to basanite ($CaSO_4 \cdot \frac{1}{2}H_2O$) within this temperature range.

The sample with a high gypsum content closely mimicked the reagent grade gypsum. Some water was lost at 30°C and at 40°C, which was determined to be the free water loss. Additional water was lost between 40°C and 50°C, and then the weight remained stable until between 70°C and 80°C. According to Herrero et al. (2016), as a precaution, oven-drying for the removal of free water should never exceed 40°C. For this study, samples were dried at 40°C, until uniform weight was obtained, to eliminate free water. Between 100°C and 110°C more water was lost, and the weight remained stable afterwards. The total weight lost at this temperature range for the reagent gypsum was 20.5%, which corresponds approximately to the total water weight expected in gypsum. Further tests carried out showed that at 105°C, the same amount of water was lost. Hence, temperature limits for this study were set at 40°C for removal of free water and 105°C for removal of bound water.

The sample with the low gypsum contents did not have the same drying pattern as the other two samples. Hence, we concluded that the thermogravimetric method for gypsum determination was more accurate for samples with higher gypsum concentrations.

The percentage of water from gypsum in each sample can be calculated by:

% water = $\dfrac{\text{Weight of water (g)}}{\text{Weight of sample (g)}}$ * 20.93

Where:

Weight of sample is the weight of the sample dried at 40°C

Weight of water = weight of sample (at 40°C) – weight of sample (at 105°C).

20.93 represents the percentage of bound water content in gypsum by mass.

Subsequently the percentage of gypsum can be calculated by:

% gypsum = $\dfrac{\text{% Water}}{20.93}$ * 100

This formula was applied to each sample to calculate the gypsum concentration in percentage per sample.

Gypsum Calculation

Wet Chemical Analysis

Gypsum concentration information from this method was originated from the reported commercial laboratory. Data for the twenty randomly selected samples are reported in Appendix 1.

X-Ray Fluorescence

Correlation analysis was carried out to determine relationship between sulfur and calcium concentrations obtained from XRF method, and the gypsum obtained from thermogravimetry using all the field samples. It was also used to determine which of the

main constituent elements in gypsum (sulfur or calcium) more closely translates to

gypsum concentration in the soil. Table 3 shows the correlation coefficient obtained

using the sulfur and calcium concentrations obtained from XRF. A strong correlation was

found between the concentration values for sulfur and calcium obtained from XRF, and

the gypsum concentration determined by thermogravimetry.

Table 2: Correlation between sulfur & calcium concentrations obtained from XRF analysis and the gypsum concentration obtained from thermogravimetry. (Surface n=241, Subsurface n=240)

Correlation Coefficients		
		Gypsum
Surface	Sulfur	0.96659
	Calcium	0.66327
Subsurface	Sulfur	0.97249
	Calcium	0.83697

Results from the correlation of both the surface and subsurface samples

indicates that while sulfur and calcium are both strongly correlated to gypsum, sulfur is

more strongly correlated than calcium. The lower correlation in calcium is thought to be

because of the presence of other calcium minerals that may be present in the samples,

such as calcite.

Hence a model was made using the gypsum concentrations obtained from the

thermogravimetric analysis and sulfur concentration from XRF, as it represents the

actual field sample population.

The gypsum calculation for this method was based on the sulfur observed in the X-ray fluorescence method as the predictor. The regression model below was used to derive the gypsum concentration for each field sample. The results are presented in Appendix 2 and 3.

Model:

Surface samples: $Y = 3.5699 + 0.0002x$

Subsurface samples: $Y = 4.1172 + 0.0003x$

Where Y is the gypsum concentration and x is the sulfur concentration

Thermogravimetry

The calculation of the gypsum concentrations in the soil sample for this method was based on the water loss during the heating process as detailed in the Laboratory Analysis section. The results are presented in Appendix 2 and 3.

Geostatistical Analysis

GIS maps were developed to highlight areas with statistically high gypsum concentrations. The Hot Spot Analysis tool on ArcGIS was used to identify spatial clusters of high concentration values of gypsum. This tool marks out areas with statistically significant high or low spatial clusters of concentrations, with 90%, 95% and 99% confidence levels. It does this using the Getis-Ord Gi* statistic, and produces results as z-score and p-value. A high z-score and small p-value for a feature indicates a spatial cluster of high values (i.e. a significant hot spot). A low negative z-score and small p-

value indicates a spatial cluster of low values (i.e. a significant cold spot). The higher (or lower) the z-score, the more intense the clustering. A z-score near zero means no spatial clustering.

Gypsum concentrations obtained from sampling were displayed on each corresponding location to obtain the gypsum concentration maps. The hotspot analysis was done using the gypsum concentration at each location as the input field. The hotspot analysis was conducted on the outcomes from x-ray method and thermogravimetric method respectively, with the results presented in map context. The resulting map highlighted areas with a cluster of significantly high percentages of gypsum, with confidence levels of between 90 to 99%. For this study, less than 40% gypsum is regarded as low range, 40 to 70% as medium, and 70% and above as high. These ranges are earmarked according to engineering specifications.

Based on the gypsum concentrations obtained from sampling along the road route, predictions on the gypsum contents of the surrounding areas were made. A buffer distance of 1000m was marked around each point and dissolved to form a solid area around all sampling points. An Inverse Distance Weighted (IDW) map was made using the obtained concentrations and the IDW prediction tool was used to further extrapolate data. Concentrations were categorized and displayed as 1-10%, 10-40%, 40-70% and >70% gypsum.

Statistical Analysis

In order to compare the soil gypsum between the subsurface and surface layers, the correlation coefficient was calculated based on all of the field samples. An analysis of variance (ANOVA) test was conducted to determine if there is any significant difference in the soil gypsum between the two layers, subsurface and surface. The correlation coefficient and ANOVA tests were conducted twice, one on the reading from the XRF, and the other on the thermogravimetric method.

To compare the three different methods of measuring gypsum in soils, data of the 20 samples sent for the wet chemistry analysis were used. For each sample location, readings from the three measuring methods were compiled for an ANOVA to determine if there is significant difference in measuring gypsum between the three methods. This one-way ANOVA was conducted twice, one for subsurface samples and the other for surface samples, at the level of significance set for $P \leq 0.05$.

Assuming readings from the thermogravimetric method are most accurate, data from the XRF method and data from the wet chemical method for the same 20 locations were used to calculate root mean square error (RMSE). The goal was to determine which method, XRF or wet chemistry, results in gypsum concentration values closer to those obtained from thermogravimetry.

RESULTS AND DISCUSSIONS

Using the reagent-grade gypsum as a standard, the wet chemical method was observed to underestimate gypsum concentrations by about 10%, while the thermogravimetric method was found to underestimate gypsum by about 4%.

The models developed using the XRF readings were observed to overestimate gypsum in soils with very low gypsum contents (<50g/kg) and underestimate the gypsum concentrations in soils with a high gypsum content as observed from the thermogravimetric method. Therefore, the model built using the sulfur observed in XRF and the gypsum observed in drying was used as the best model in calculating soil gypsum in the XRF method.

Gypsum has a bound water content of 20.9% by mass corresponding to 209g water per kilogram gypsum. Water content in the subsurface samples ranged from a low of 1.8g/kg to a high of 197g/kg, and from a low of 1.9g/kg to a high of 186.4g/kg in the surface samples.

Surface Samples

The gypsum contents at the surface were lower compared to those at the subsurface. This is thought to be as a result of chemical leaching by rainwater. About half of the surface locations sampled had gypsum concentrations of less than 50g/kg i.e., less than 5% gypsum and 77% of locations had gypsum concentrations less than

100g/kg. 93.75% of sampling locations had gypsum concentrations less than 400g/kg, with only 15 locations over 400g/kg gypsum concentration and 3 locations over 700g/kg. A summary of results obtained is shown in Table 5. Figures 13 and 14 show that the majority of the results obtained gypsum concentrations of 100g/kg or less. A geographic representation of the results using both methods is shown in Figures 15, 16 and 17, with Figures 16 and 17 highlighting cluster areas with high gypsum contents.

Table 3: Summary statistics for surface samples (n=239).

	Mean	Std Dev	Minimum	Maximum
Sulfur (g/kg)	29.836	59.507	0.047	278.429
Calcium (g/kg)	94.013	47.065	0.077	253.256
Water content from thermogravimetry (g/kg)	23.437	33.042	1.955	186.376
Gypsum from XRF (g/kg)	97.698	123.212	36.967	592.557
Gypsum from thermogravimetry (g/kg)	109.176	152.304	9.359	891.754
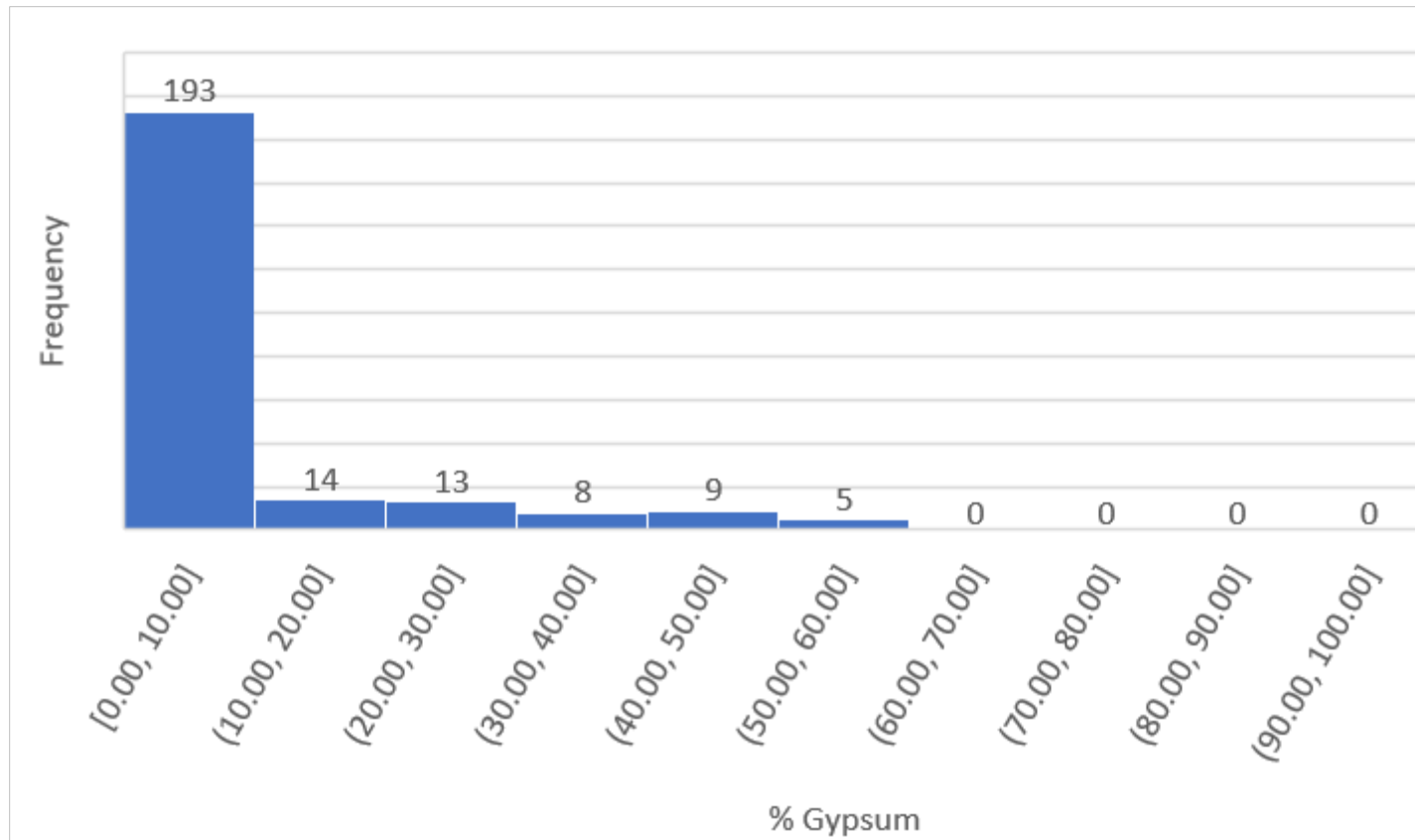
Figure 6: Frequency distribution of gypsum concentrations obtained using the XRF analysis method for surface samples.
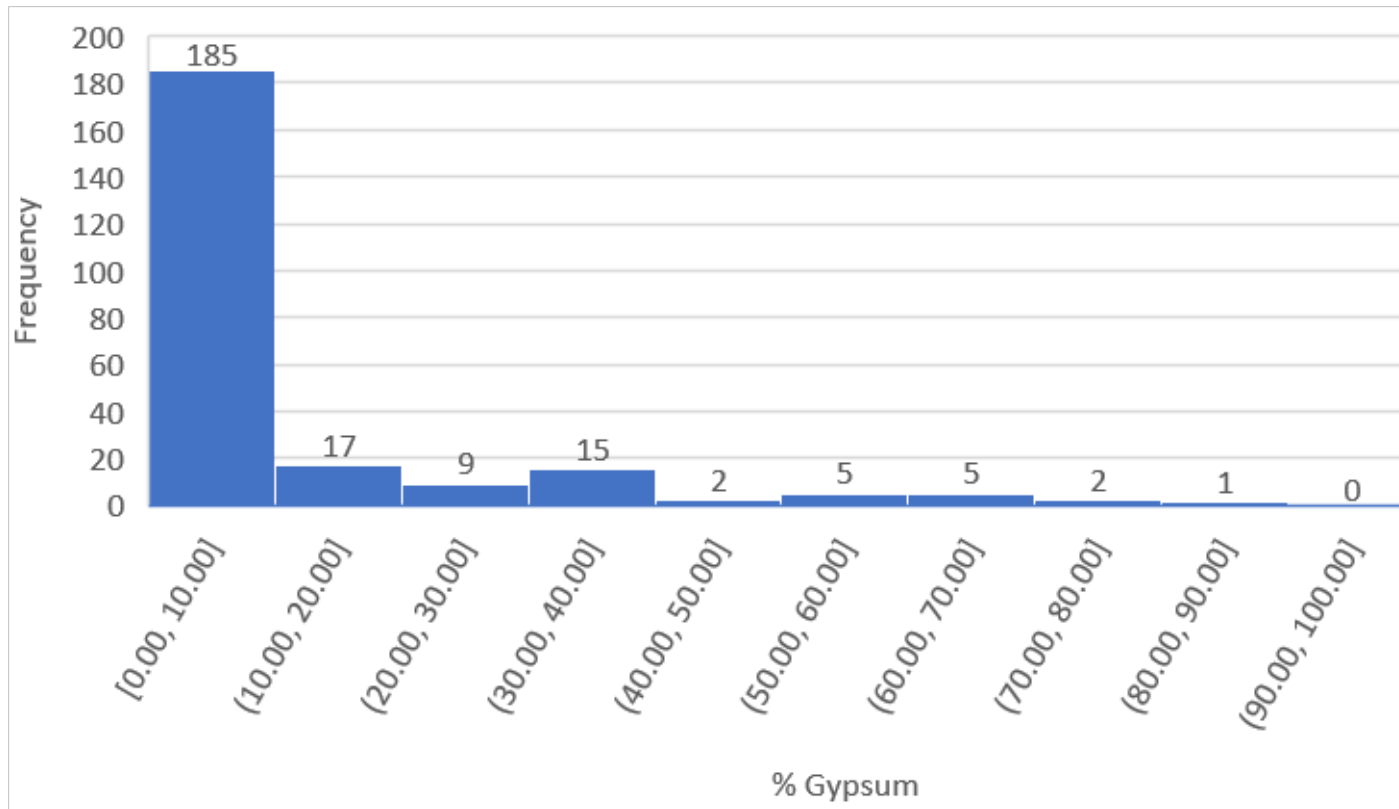
Figure 7: Frequency distribution of gypsum concentrations obtained using the thermogravimetric method for surface samples.
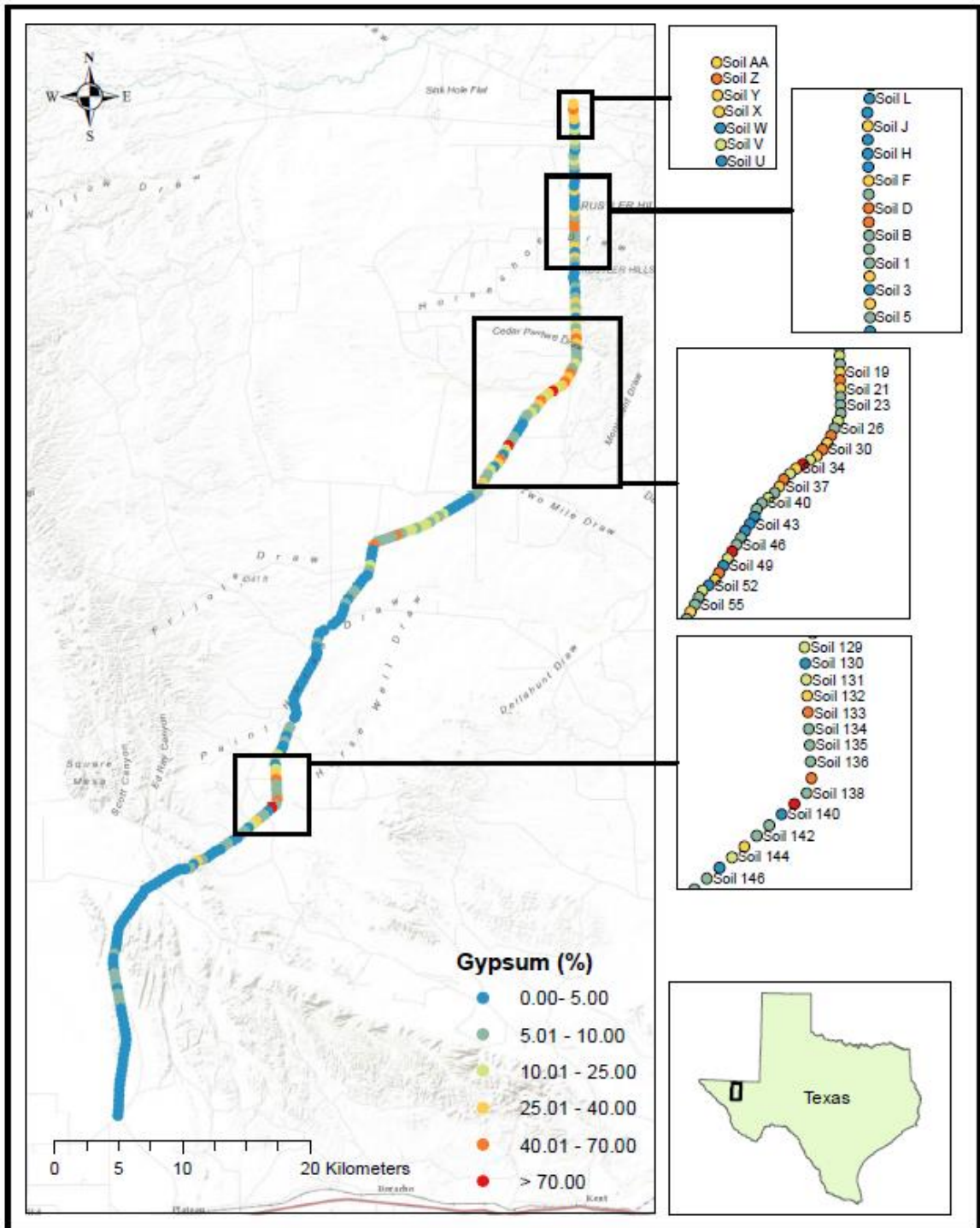
Figure 8: Map showing gypsum concentrations of surface samples using thermogravimetric method along the proposed road route.
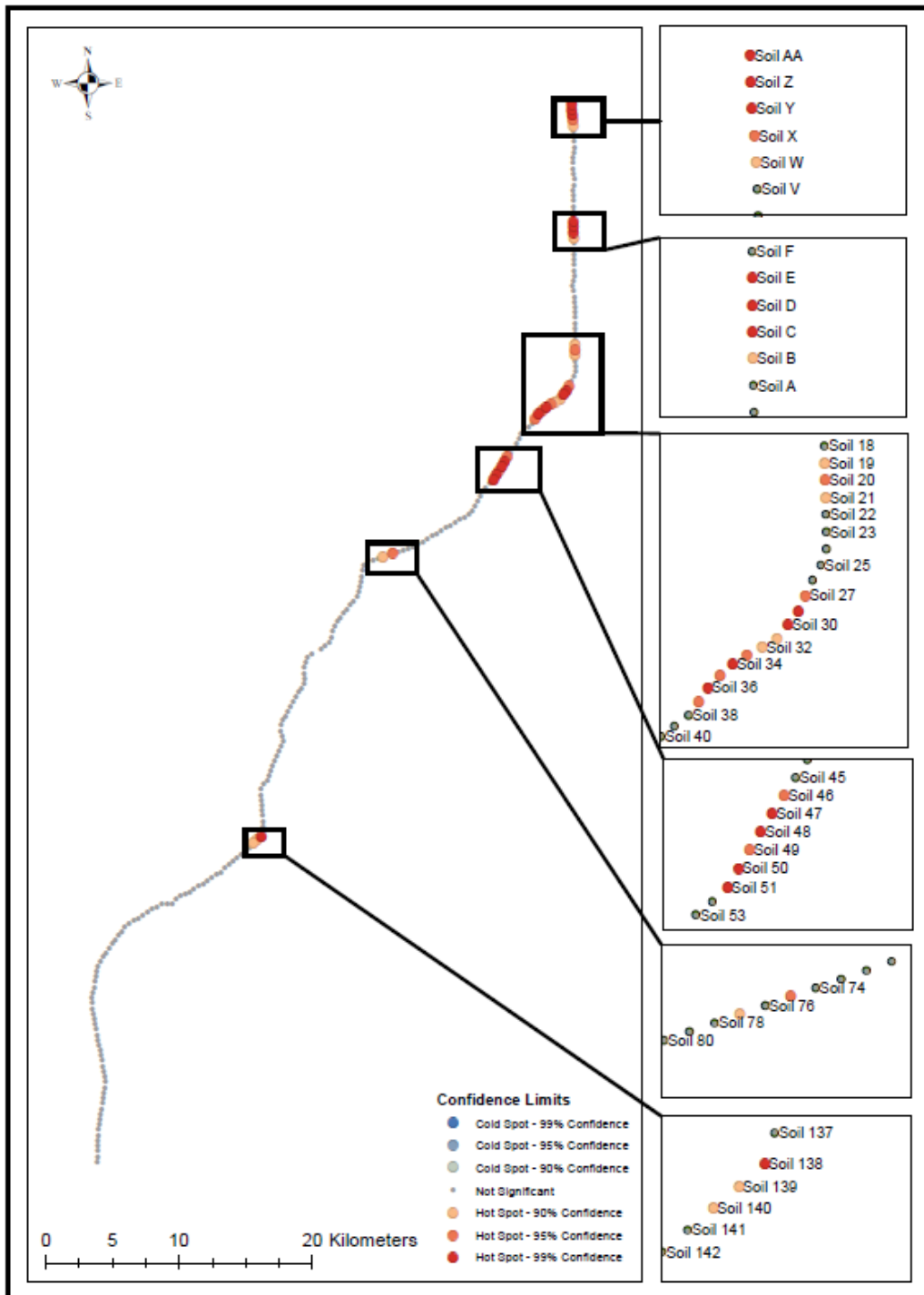
Figure 9: Hotspot analysis highlighting cluster areas in the surface samples with high gypsum concentrations obtained from XRF analysis.
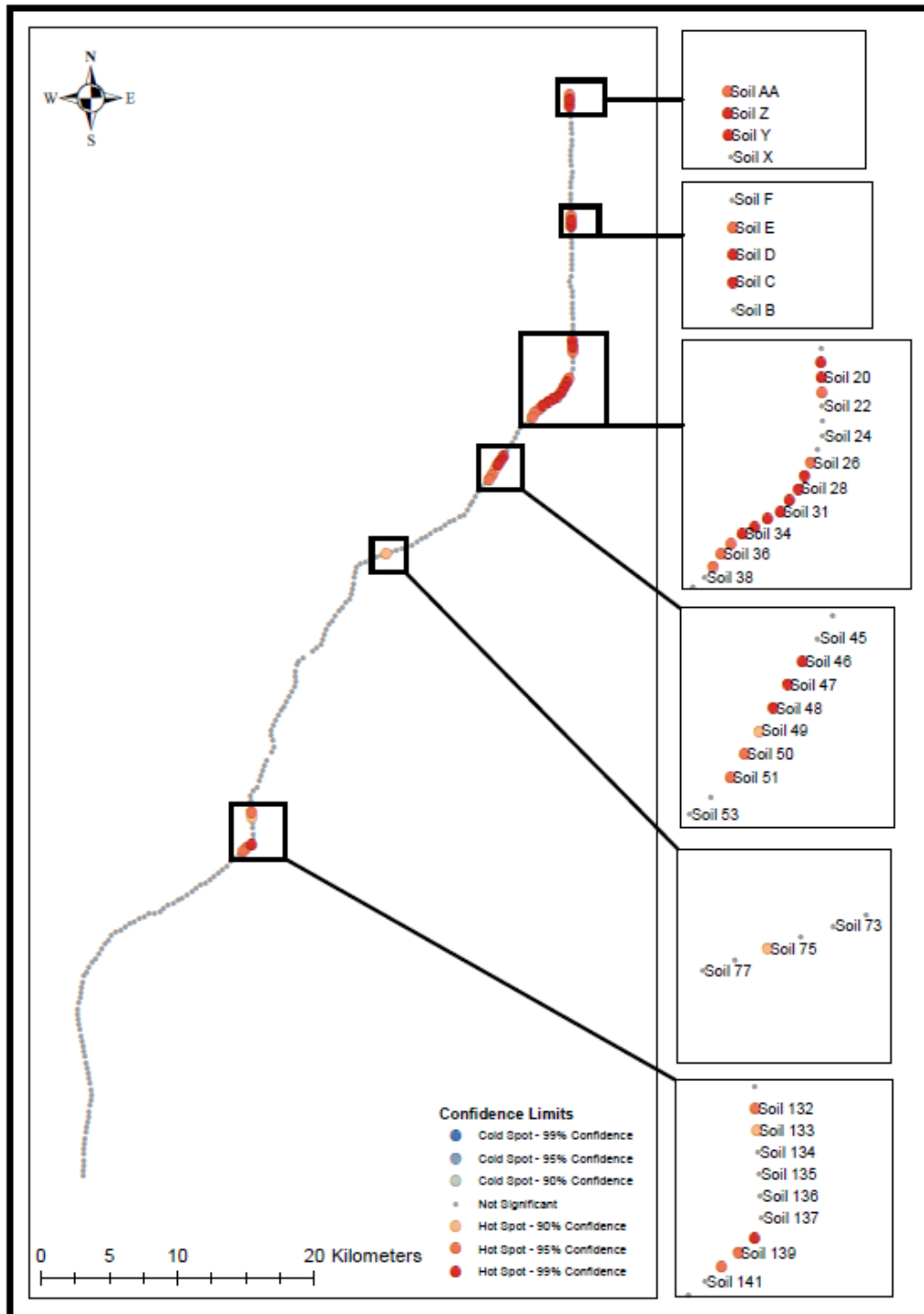
Figure 10: Hotspot analysis highlighting cluster areas in the surface samples with high gypsum concentrations obtained from thermogravimetric analysis.
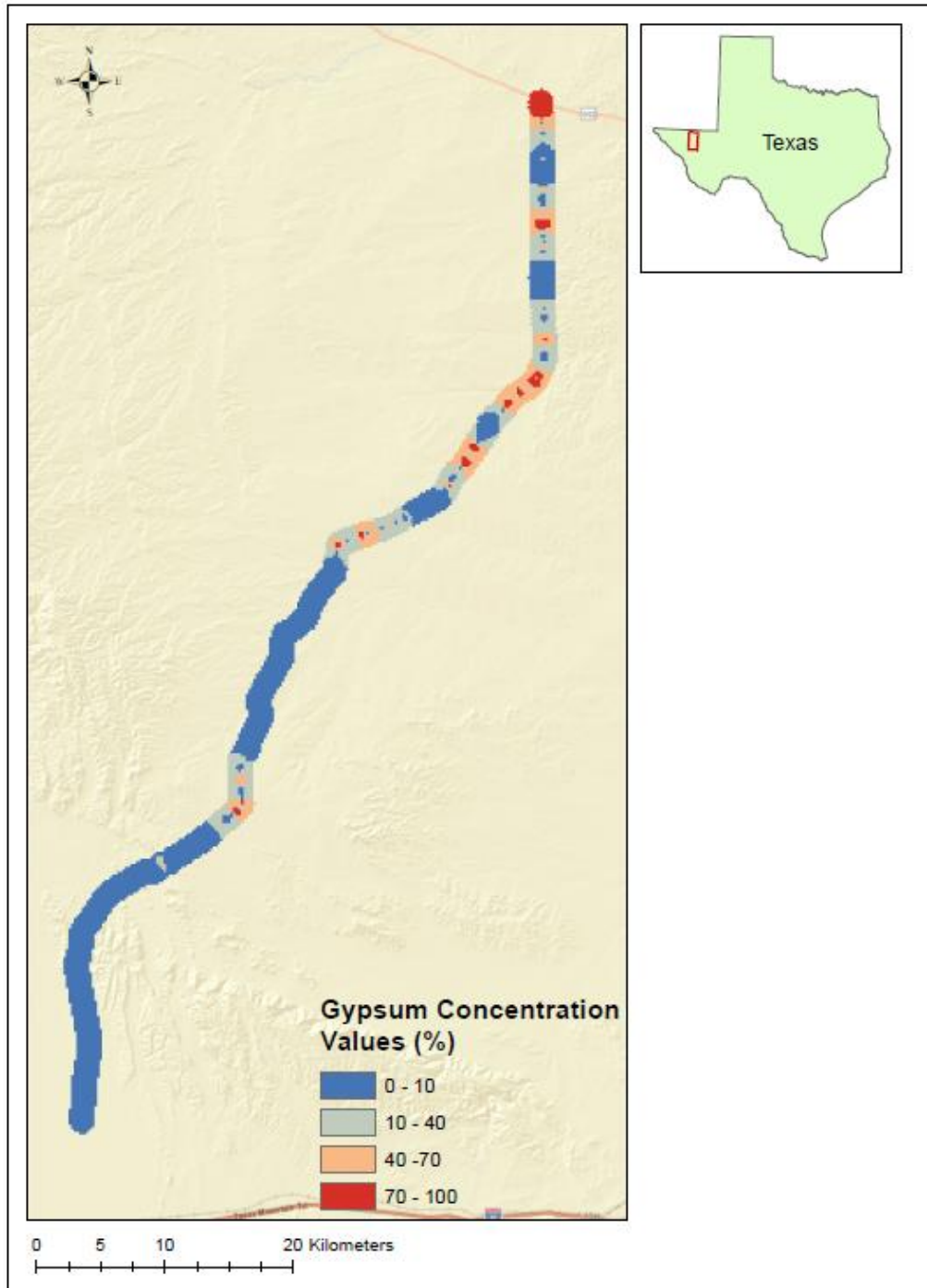
Figure 11: IDW prediction of gypsum contents in soils within 1000m from the proposed road route. Predictions made using concentrations obtained from XRF analysis of the surface samples
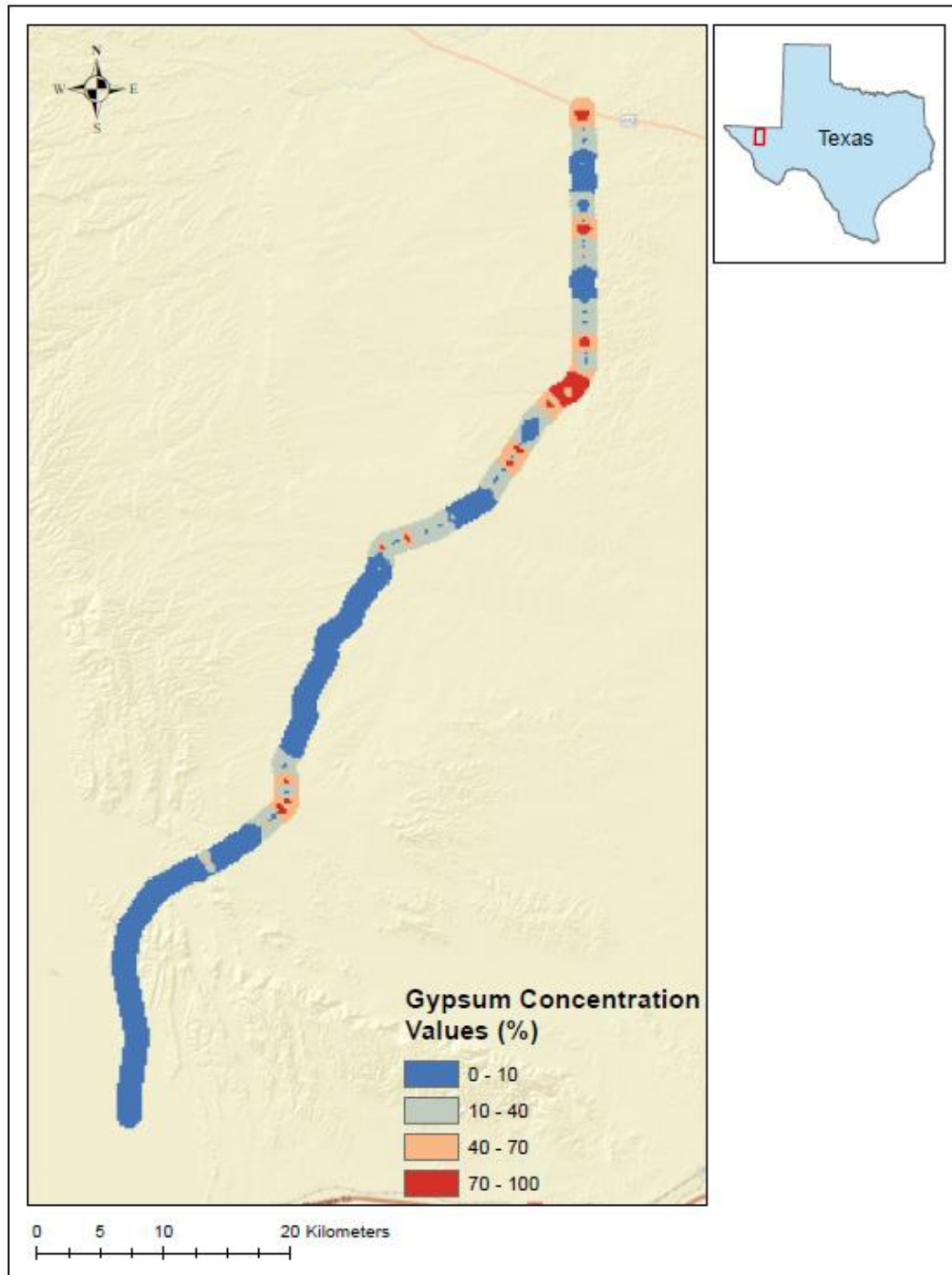
Figure 12: IDW prediction of gypsum contents in soils within 1000m from the proposed road route. Predictions made using concentrations obtained from thermogravimetric analysis of the surface samples.

Results from the hot spot analysis shows significant clusters of high gypsum concentrations, with scattered cold spots where the gypsum concentrations were relatively low. Therefore, we were able to delineate areas with high gypsum concentrations.

Subsurface Samples

The summary statistics for the subsurface samples is shown in Table 4. The mean gypsum content of the samples obtained from XRF analysis was slightly higher than that obtained from thermogravimetry. Of the points sampled, about 65.5% had gypsum concentrations less than 100g/kg, with about three-quarters of this being less than 50g/kg i.e., 5% gypsum; 10.8% had concentrations between 100 and 300g/kg, 12.9% had concentrations between 400 and 700g/kg, and 10.8% had concentrations of over 700g/kg. Soil sample sites 145 to 215, by Luckett Draw extending south to the end of the road right-of-way, and 84 to 127 by Emory Draw and extending southwards, has low gypsum concentrations, with an average of 42g/kg and 58g/kg gypsum respectively. This translates to about half of the subsurface samples not having a gypsic or petrogypsic horizons.

There were several clusters of sampling points with soils rich in gypsum, the largest of them occurring between sampling sites 19 and 39, with the average gypsum concentration being 586.5g/kg, and 50% of the soils in this range having gypsum concentrations above 700g/kg. A smaller cluster occurred between sampling sites 71

and 76, with the average gypsum concentration being 622.8g/kg, and 83% of the soils

having concentrations greater than 700g/kg. Figures 8 and 9 shows that majority of the

samples have gypsum concentrations of 100g/kg or less, when measured using both the

XRF and thermogravimetry methods. A spatial distribution of gypsum contents

measured using both methods is shown in Figures 10, 11 and 12, with Figures 11 and 12

highlighting cluster areas with high gypsum contents.

Table 4: Summary statistics for subsurface samples (n=239).

	Mean	Std Dev	Minimum	Maximum
Sulfur (g/kg)	65.442	100.324	0.636	304.062
Calcium (g/kg)	118.887	65.005	4.661	288.493
Water content from thermogravimetry (g/kg)	45.570	58.272	1.831	197.118
Gypsum from XRF (g/kg)	237.498	300.974	43.079	953.359
Gypsum from thermogravimetry (g/kg)	218.038	278.812	8.7612	943.148
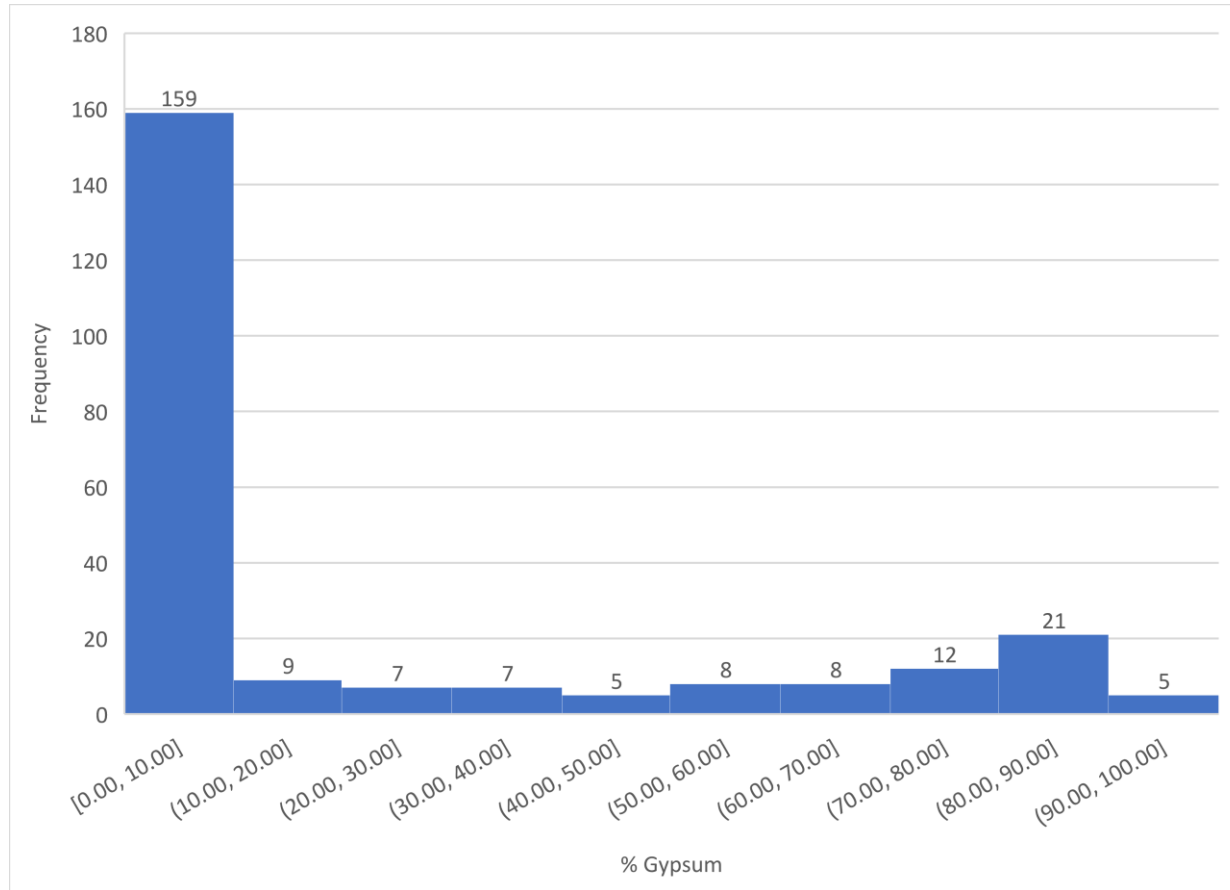
Figure 13: Frequency distribution of gypsum concentrations obtained using the XRF method for subsurface samples.
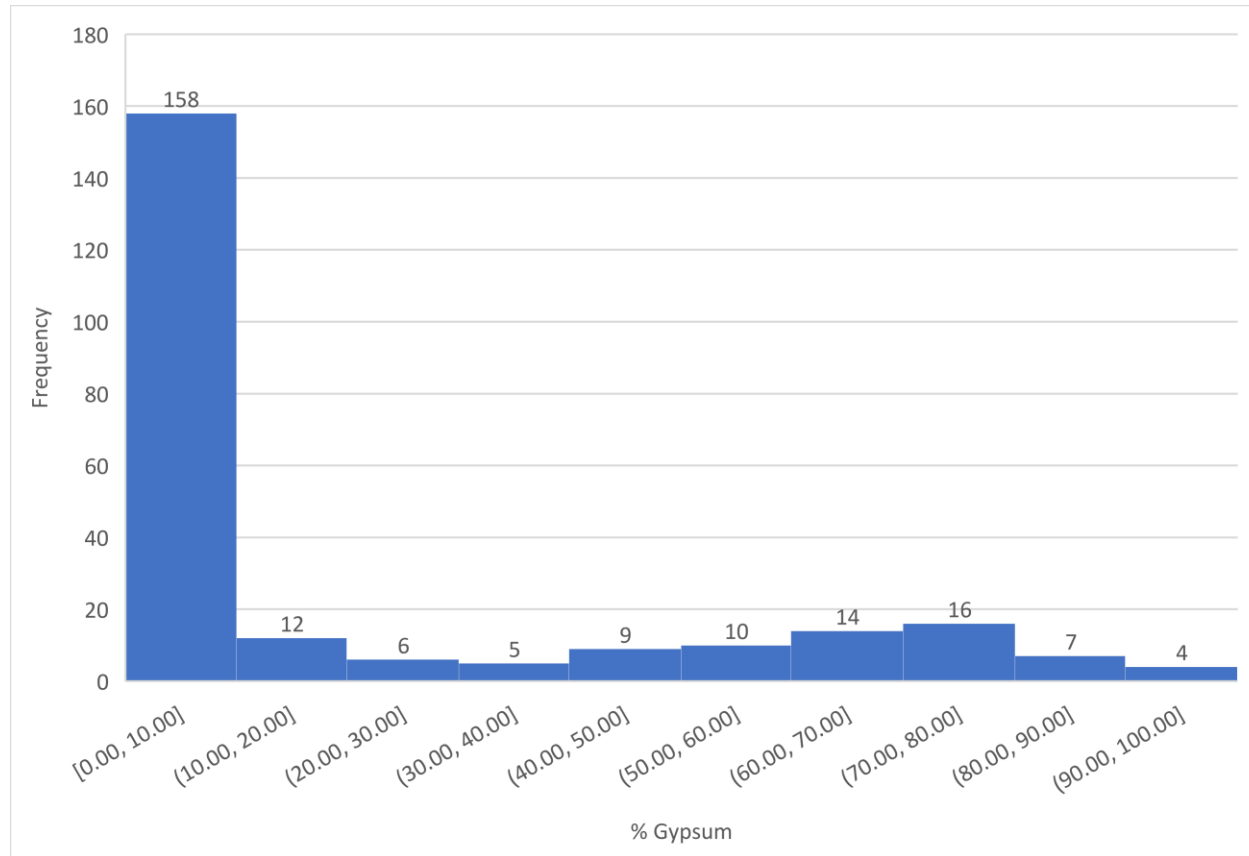
Figure 14: Frequency distribution of gypsum percentages obtained using the thermogravimetric method for subsurface samples.
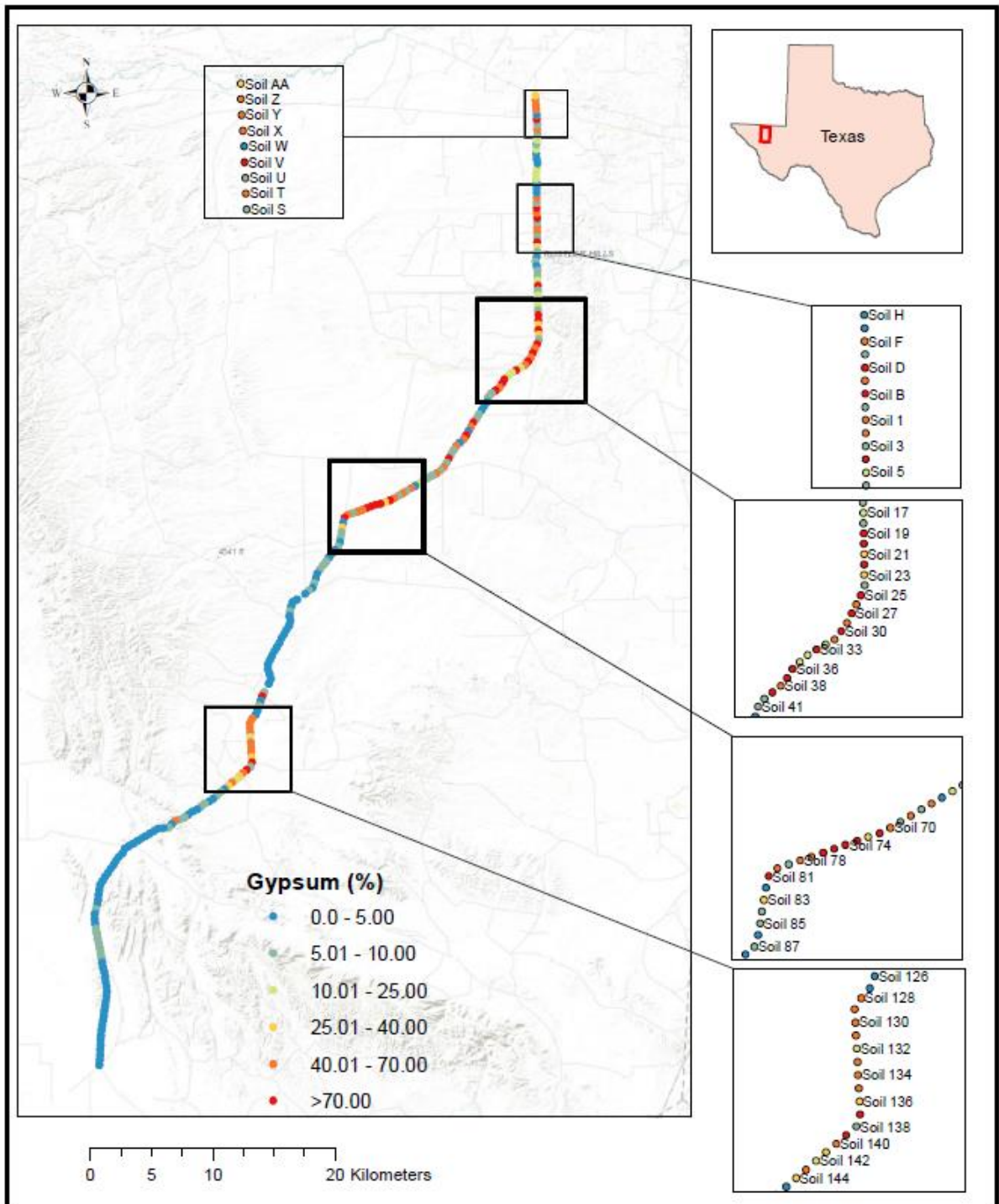
Figure 15: Map showing gypsum concentrations, obtained from thermogravimetry, of subsurface samples along the proposed road route.
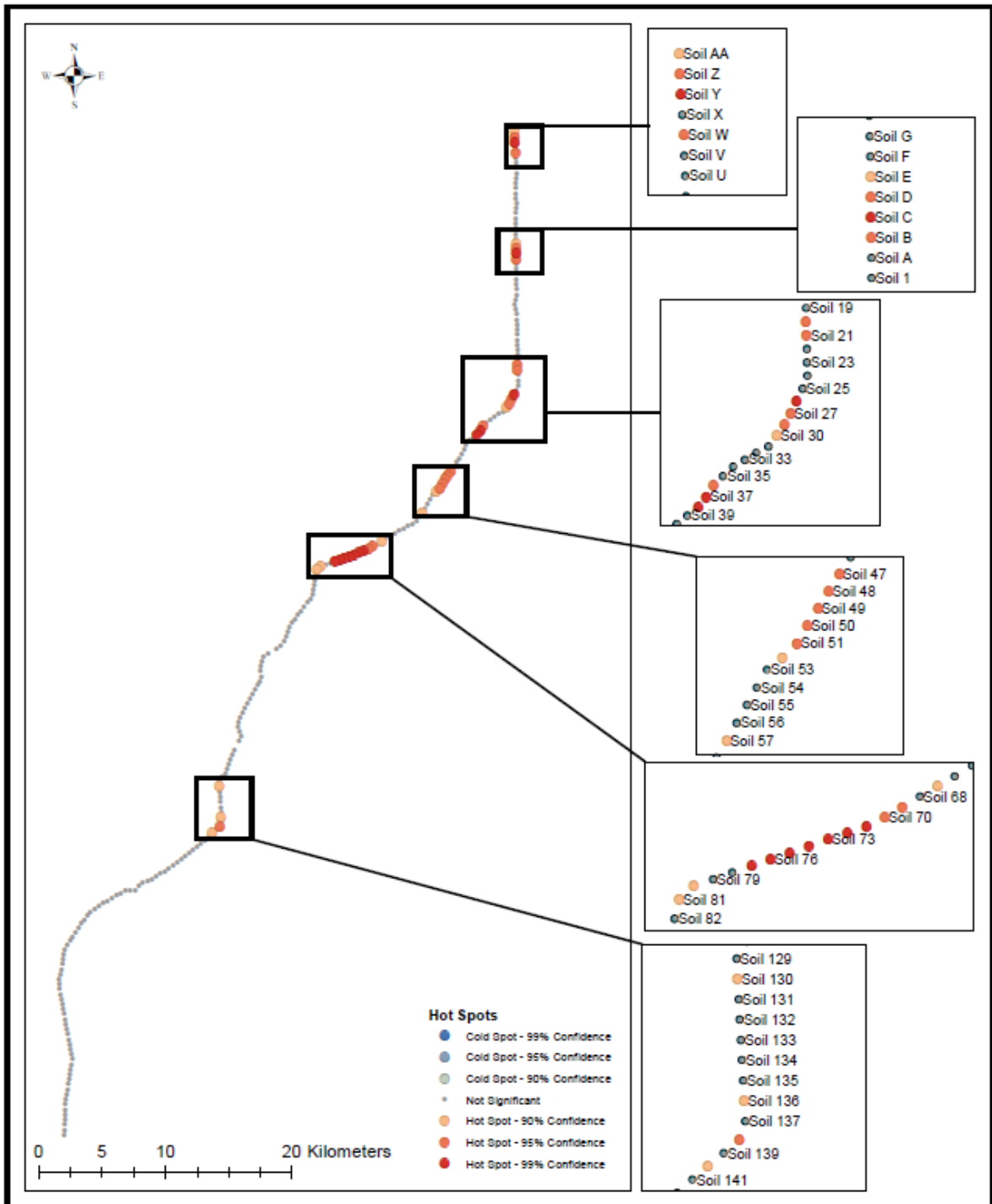
Figure 16: Hotspot analysis highlighting cluster areas in the subsurface with high gypsum concentrations obtained from XRF analysis.
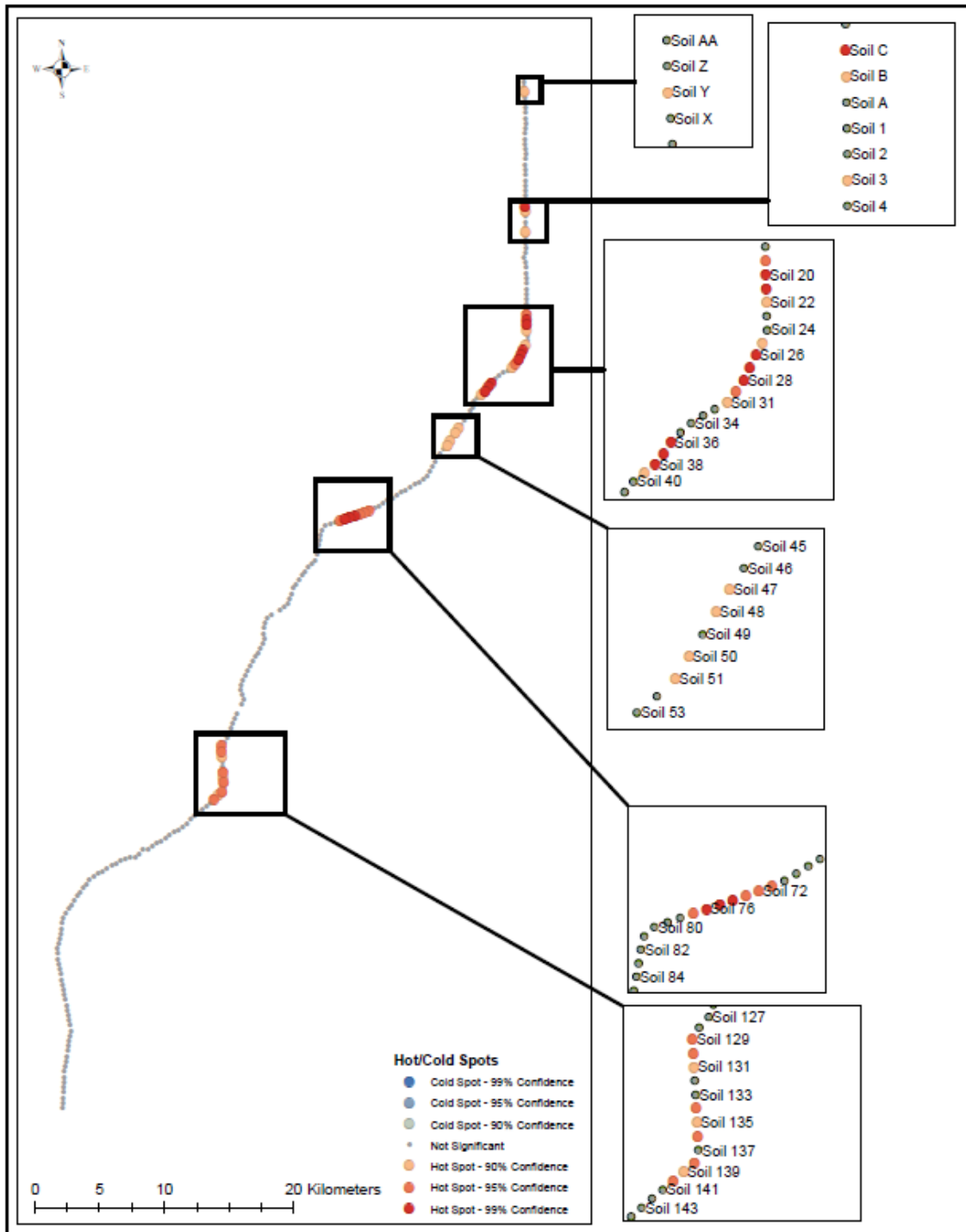
Figure 17: Hotspot analysis highlighting cluster areas in the subsurface with high gypsum concentrations obtained using thermogravimetric analysis.
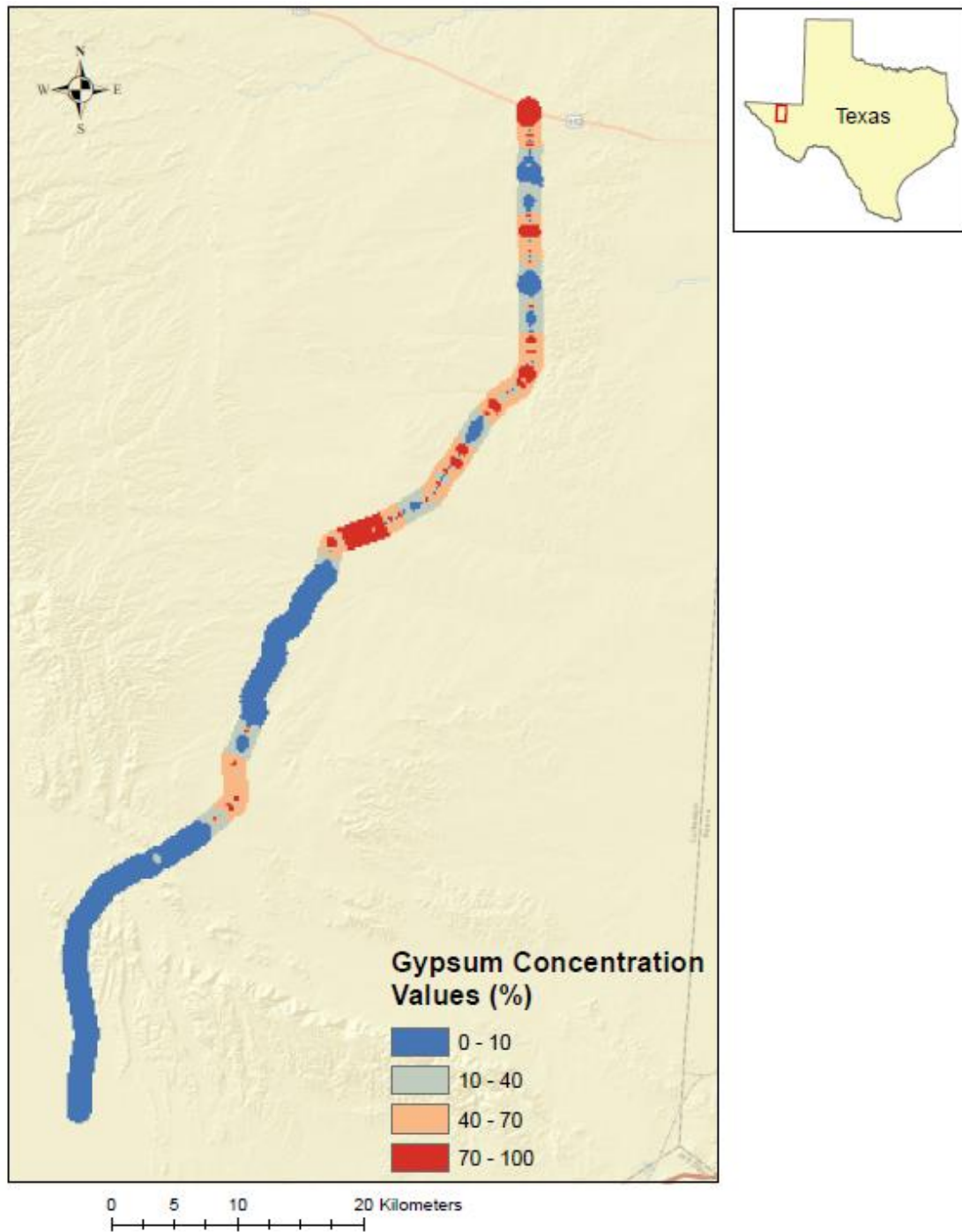
Figure 18: IDW prediction of gypsum contents in soils within 1000m from the proposed road route. Predictions made using concentrations obtained from XRF analysis of the subsurface samples.
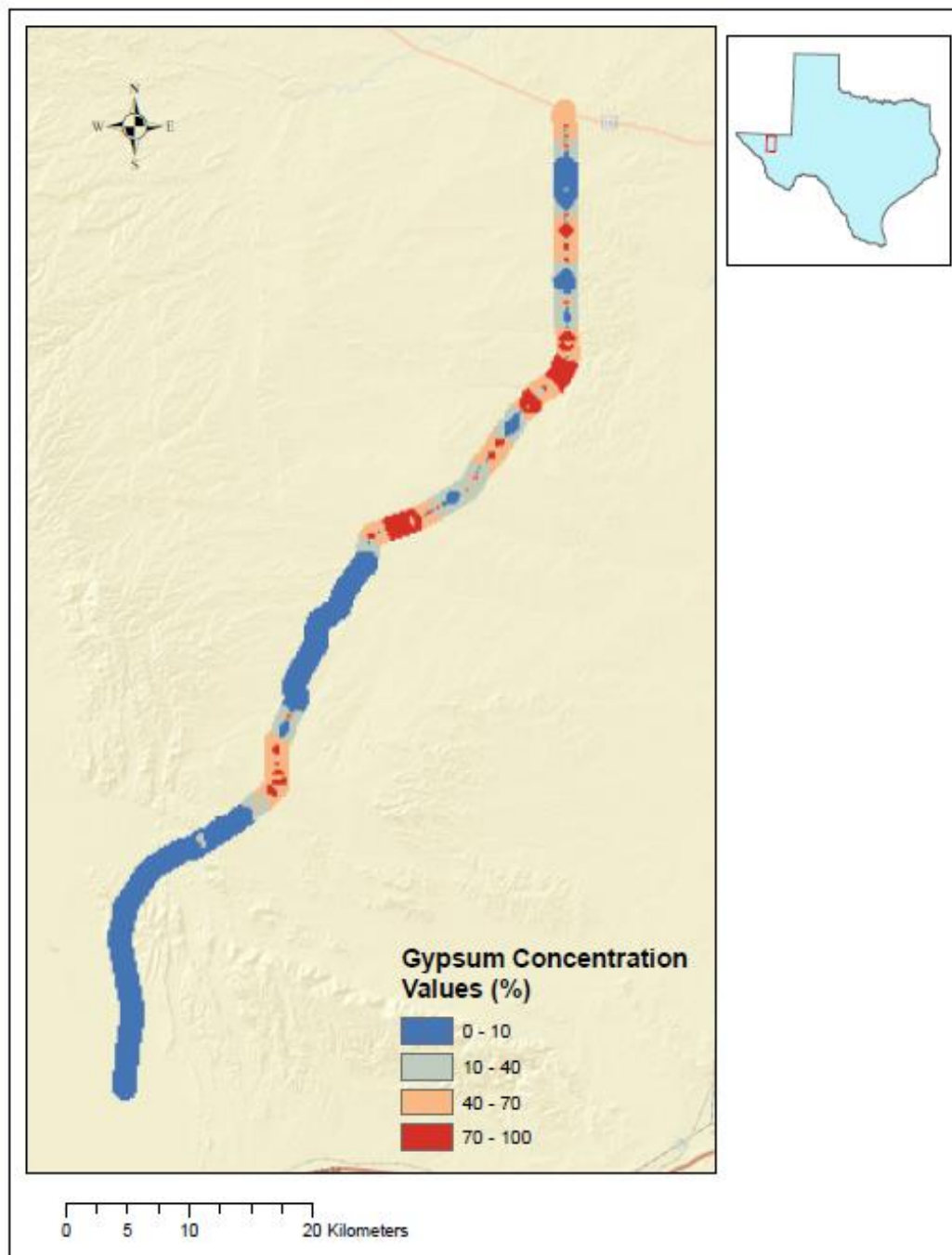
Figure 19: IDW prediction of gypsum contents in soils within 1000m from the proposed road route. Predictions made using concentrations obtained from thermogravimetric analysis of the subsurface samples.

Comparing the frequency distributions for data obtained from both

thermogravimetric and XRF analysis, we can see that the XRF analysis returns higher

concentration values compared to the thermogravimetric method. This agrees with the

mean gypsum concentrations found in Table 4. Despite this however, the hotspot areas

are consistent for both gypsum measurement methods. This represents similarities in

the results for measuring gypsum in soils using either method.

Some locations were identified that have high gypsum concentrations in both

the surface and subsurface layers. More attention should be paid to these areas, as the

high gypsum contents, under the right conditions, can easily dissolve creating voids

which can be detrimental to engineering structures. Listed in the Appendix 4 are the

locations of clusters along the proposed road route with notably high gypsum contents.

Surface and Subsurface Comparison

The ANOVA procedure was used to determine if there was a significant

difference between surface and subsurface concentrations of gypsum using the XRF and

thermogravimetric methods. The level of significance (α-value) was set at 0.05. The

results are returned as a probability (P value). A P value less than 0.05 signifies a

significant difference while a P value greater than 0.05 signifies no significant difference

in the test samples. P-values of <0.0001 was obtained in both instances signifying that

there is a significant difference between surface and subsurface gypsum concentrations.

Table 5: Comparison of surface and subsurface concentrations from XRF method. (n=481)

Source	DF	Sum of Squares	Mean Square	F Value	Pr > F
Model	1	2339939.89	2339939.89	44.45	<0.0001
Error	479	25218382.44	52647.98		
Corrected Total	480	27558322.33			

Table 6: Comparison of surface and subsurface concentrations from thermogravimetric method. (n=480)

Source	DF	Sum of Squares	Mean Square	F Value	Pr > F
Model	1	1339706.48	1339706.48	26.18	<0.0001
Error	478	24465046.62	51182.11		
Corrected Total	479	25804753.11			

Using the XRF method, the mean concentration of the surface samples was

97.7g/kg while the mean for the subsurface samples was 237.5g/kg. Also, using the

thermogravimetric method, the mean concentration of the surface samples was

109.2g/kg while the mean for the subsurface samples was 218g/kg. From these, it can

be seen that the mean concentrations of the subsurface samples were significantly

higher than the mean concentrations of the surface samples.

This significant difference can be attributed to leaching. Brenner et al. (1981)

defines leaching in soils as a process which removes materials in solution (e.g. salts,

evaporites) and cementation agents from a section of a soil profile. Therefore, there has

to be a solvent, in this case, precipitation, which dissolved some of the gypsum at the

surface. However, due to the low amounts of precipitation in the Gypsum Plain, the flow

is thought to be limited and thus does not travel far, thereby depositing the dissolved

gypsum in the subsurface. This may be a reason for the higher gypsum contents in the

subsurface compared to the surface soil samples. Figure 18 shows the relationship

between the two depicting a low correlation. According to Ahmad et al. (2012), leaching

increases soil compressibility, as it dissolves the soluble materials thereby increasing

voids.
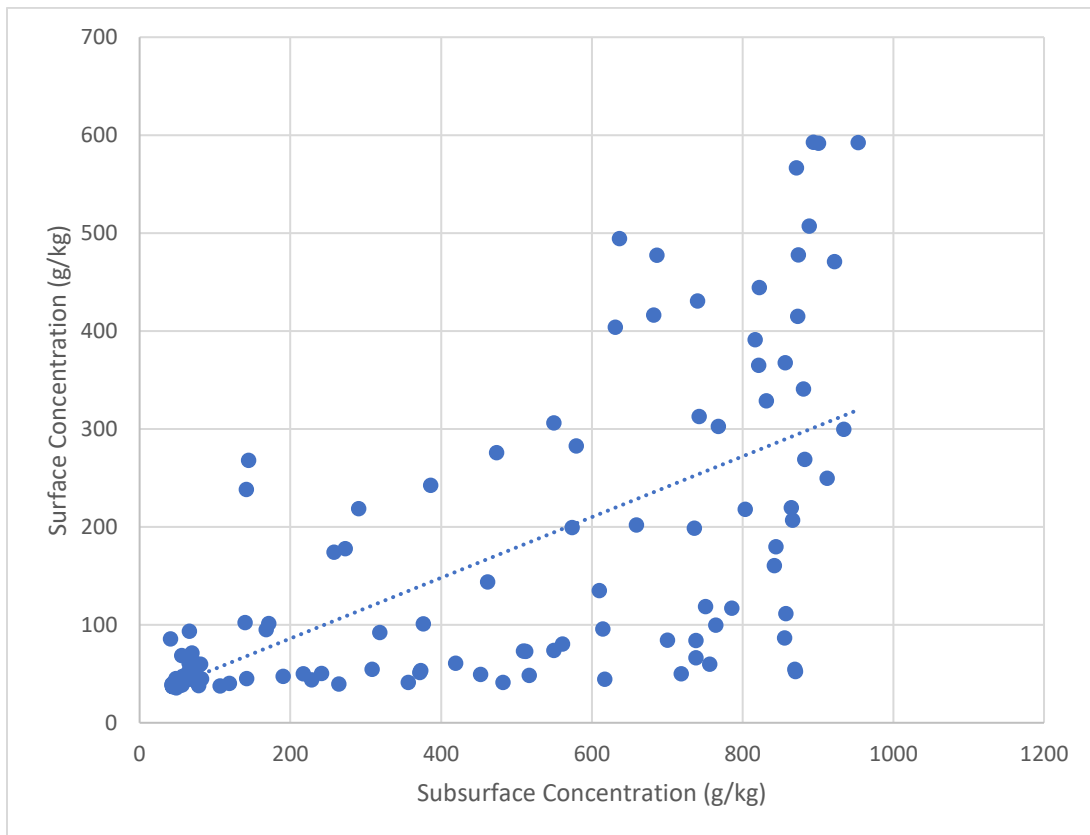
Figure 20: Cross-plot showing the relationship between surface samples and subsurface samples for XRF. The trendline generally shows an increase in subsurface concentration as the surface concentration increases (r^2= 0.57, n=240)
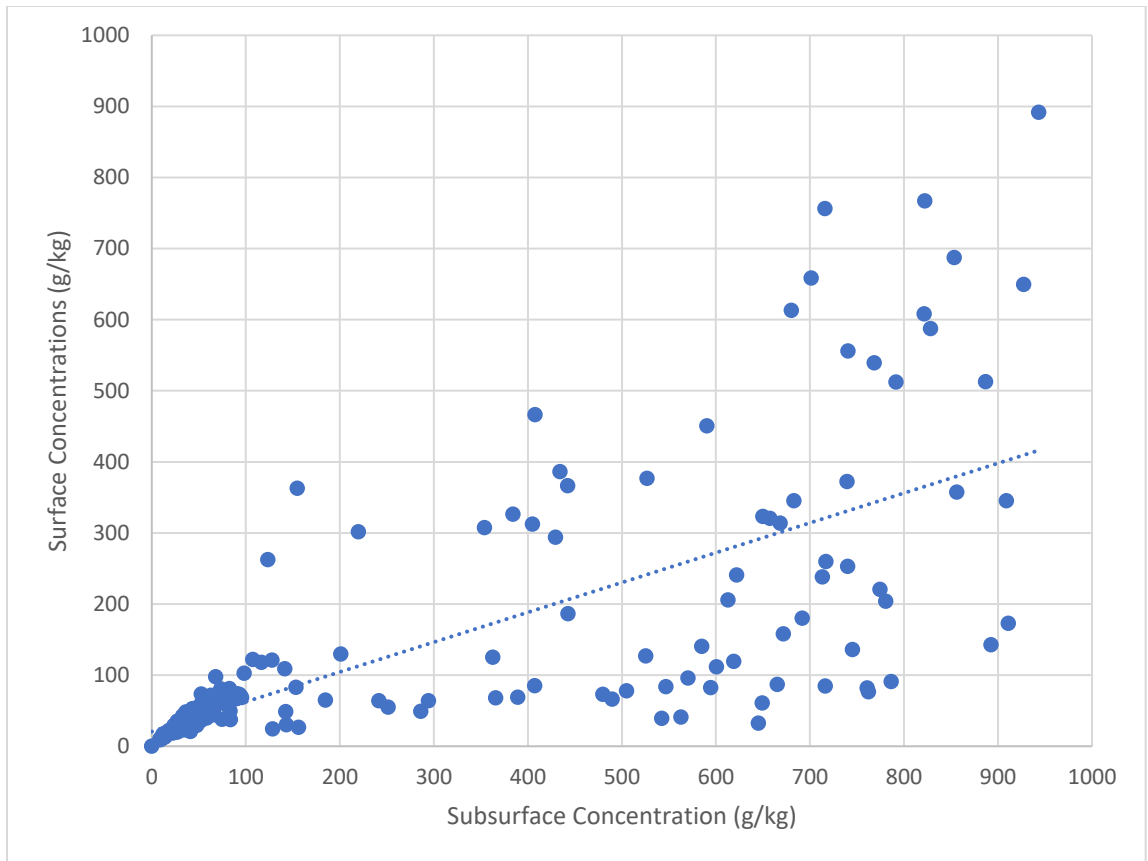
Figure 21: Cross-plot showing the relationship between surface samples and subsurface samples for thermogravimetry. The trendline generally shows an increase in subsurface concentration as the surface concentration increases (r^2= 0.55, n=240)

Comparison of the Three Methods

Results obtained from the wet chemical, XRF and thermogravimetric methods were compared for the twenty randomly selected samples from the surface and subsurface using the ANOVA procedure, to determine if there was a significant difference between the gypsum concentrations obtained using the XRF, thermogravimetric and wet chemical methods.

A P- value of 0.7712 was obtained for the surface samples (Table 8) while 0.8851 was obtained for the subsurface samples (Table 9) in the test. Therefore, we can conclude that there is no significant difference between the gypsum concentrations obtained from the XRF, thermogravimetric and wet chemical methods.

Table 7: Comparison of gypsum concentrations between the three methods using surface samples (n=30)

Source	DF	Sum of Squares	Mean Square	F Value	Pr > F
Model	2	49.541147	24.770573	0.26	0.7712
Error	27	2549.735800	94.434659		
Corrected Total	29	2599.276947			

Table 8: Comparison of gypsum concentrations between the three methods using subsurface samples (n=30)

Source	DF	Sum of Squares	Mean Square	F Value	Pr > F
Model	2	210.19992	105.09996	0.12	0.8851
Error	27	23138.89688	856.99618		
Corrected Total	29	23349.09680			

The RMSE was computed for the XRF and wet chemical methods against the thermogravimetric method. Thermogravimetric method was chosen because it had the least observed error using the reagent-grade control sample. RMSE for the XRF method was 4.6 while that for the wet chemistry method was 6.4. If the thermogravimetric method attained the most accurate readings for gypsum concentration, the XRF would be more accurate than the wet chemical method.

CONCLUSION

In road construction over an area with gypsic soils, such as in the Gypsum Plain, it is important to identify areas with very high concentrations of gypsum, as they are more prone to the development of associated hazards. Three different methods were used to quantify gypsum in the study area. Thermogravimetry, wet chemical and portable X-ray fluorescence methods were compared in measuring gypsum in soils. It was found that there is no significant difference in the results obtained between the three methods. However, the high cost and time involved for the wet chemical method prevents it from being applied to a large sample size. Another limitation of the wet chemical method is that the calcium or sulfate concentrations obtained may also include ions from other calcium and sulfate containing compounds present in the soil sample. The thermogravimetric method on the other hand comes with a lower cost but requires a longer amount of time to ensure that the samples are properly dried at the appropriate temperatures. This method does have limitations for analyzing soil samples with low gypsum content (Arteida et al., 2006), because it is based on determining water content of gypsum. The portable XRF method is the fastest that can be used directly in the field for attaining readings. However, since the model for calculating gypsum concentrations is specific to a given set of samples, a representative model will have to be developed in order to accurately represent population studies. Temperature

conditions in the field in semi-arid regions closely relate to drying conditions for free water removal, therefore, it eliminates the need for oven-drying to remove free water when using XRF for field sampling.

In this study, sampling was conducted over a distance of about 96.5km, including areas of the proposed road route and existing roads. The main engineering limitations of gypsic soils are iron corrosion, sinkholes, subsidence by karstification, as well as the reaction of the sulfates present in gypsum with concrete and other building materials (Herrero et al., 2009). Gypsum content along the stretch of the sampled areas varies greatly with the lowest concentrations found at the south end of the sampling area. Most of the sample locations with low gypsum content occur on FM 2185. A distance of between 12 to 21km of the total sampled locations, was found to have high gypsum content. Of this, about 5km occurs on the already constructed FM 2185. The proposed road route was found to have a significantly higher gypsum content compared to FM 2185.

A limitation of this study was the inability to obtain samples over smaller distances due to time constraint and the total distance to be covered. Thus, gypsum concentrations obtained at a point were assumed to be representative of the concentrations at significant distances from the point. Also, it was assumed that the predominant soil content was gypsum in the samples and thus, the sulfur and calcium

concentrations obtained from the x-ray fluorescence method was assumed to be entirely from gypsum.

Further tests will need to be carried out, especially in the areas displaying clusters with high gypsum contents, as these areas have a high potential for developing karst features. Geophysical and geological surveying is necessary to identify existing karst features. Technologies used for geophysical studies can include ground penetrating radar which works well in dry rocks and can image down to about 20m (Cooper & Guiterrez, 2013), electrical resistivity tomography (ERT) and microgravity surveying. These approaches, together with the gypsum content of the soils, will allow for detecting the spatial distribution of the karst features and areas likely to develop these features in the surrounding areas. A GIS model can be developed and applied in places with similar soil characteristics. Thierry (2009) proposed that a model that captures the overlap between places with high gypsum concentration, places with the probability of dissolution and places with the presence of features or probability of collapse can aid in identifying areas that can be problematic.

To reduce the risk of damage to engineering structures, after determining areas with the least amount of subsidence hazards, mitigation measures have to be put in place with subsequent monitoring technology. Roads can then be reinforced with geogrids and equipped with monitoring systems.

LITERATURE CITED

Adams J.E, Cheney M.G, Deford R.K, Dickey R.I, Dunbar C.O, Hills J.M, King R.E, Lloyd E.R, Miller A.K and Needham C.E, (1939). Standard Permian of North America: American Assoc. Petroleum Geol., Bull., v.23, no 11. Pp 1673-1681.

Ahmad F., Md Said M.A., Najah L. (2012). Effect of Leaching and Gypsum Content on Properties of Gypseous Soils. International Journal of scientific and Research Publications Vol. 2, Issue 9.

Bockheim J.G. 2014 Gypsic and Petrogypsic Horizons. Soil Geography of the USA: A Diagnostic-Horizon Approach. Pp179-188. DOI 10.1007/978-3-319-06668-4_17

Buol S.W., Southard R.J., Graham R.C., McDaniel P.A. (2011). Soil Genesis and Classification- Sixth Edition. Wiley-Blackwell Publication.

Casby-Horton S., Herrero J., Rolong N.A., (2015) Gypsum Soils—Their Morphology, Classification, Function, and Landscapes. Advances in Agronomy Vol. 130, pp 231-290. DOI:10.1016/bs.agron.2014.10.002

Cooper A.H. (2002) Environmental Problems Caused by Gypsum Karst and Salt Karst in Great Britain. Carbonates and Evaporites, 17(2), 116-120.

Cooper A.H., Gutiérrez, F., (2013). Dealing with Gypsum Karst Problems: Hazards, Environmental Issues, and Planning. In: Shroder, J. (Editor in Chief), Frumkin, A. (Ed.), Treatise on Geomorphology. Academic Press, San Diego, CA, vol. 6, Karst Geomorphology, pp. 451–462.

Ford D., Williams P., (2007) Introduction to Karst in John Wiley & Sons Ltd, Karst Hydrogeology and Geomorphology. Pp 1-4 The Atrium, Southern Gate, Chichester, West Sussex PO19 8SQ, England

Gunay G. (2002) Gypsum Karst, Sivas, Turkey. Environmental Geology (2002) 42:387–398. DOI 10.1007/s00254-002-0532-0

Gunn J. (2004) Encyclopedia of Caves and Karst Science. In Fitzroy Dearborn An Imprint of the Taylor and Francis Group

Herrero J., Artieda O., Hudnall W.H. (2009) Gypsum, A Tricky Material. Soil Sci. Soc. Am. J. 73(6): 1757-1763 DOI:10.2136/sssaj2008.0224

Herrero J., Artieda O., Weindorf D.C. (2016) Methods of Soil Analysis- Soil Gypsum Determination. Soil Sci. Soc. Am. J. 82:293–294. DOI:10.2136/sssaj2017.12.0429

Hill A.E. (1937). The Transition Temperature of Gypsum to Anhydrite. J. Am. Chem. Soc. 59:2242–2244. DOI: 10.1021/ja01290a039

Hill C.A. (1996). Geology of the Delaware Basin, Guadalupe, Apache and Glass Mountains: New Mexico and West Texas: Permian Basin Section: Midland, Texas, SEPM, 480 p.

Johnson S.K. (1996). Gypsum Karst in the United States. Int. J. Speleol. 25 (3-4), 1996. p. 183-193

Johnson S.K. (2008) Evaporite-Karst Problems and Studies in the USA. Environ Geol 53:937-943 Doi 10.1007/s00254-007-0716-8

Kalnicky D.J., Singhvi R. (2001). Field Portable XRF Analysis of Environmental Samples. J. Hazard. Mater 83:93-122

Karathanasis A.D. (2008) Thermal Analysis of Soil Minerals in SSSA Book series 5 A.L. Ulery & L.R Drees, Methods of Soil Analysis Part 5-Mineralogical Methods pp 117-160, DOI:10.2136/sssabookser5.5

King P.B. (1942). Permian of West Texas and Southeastern New Mexico: American Association of Petroleum Geology, Bull., v.26 no.4, pp 535-763

Kirkland D.W., Evans R. (1980) Origin of the Castiles on the Gypsum Plain of Texas and New Mexico. In: Dickerson PW, Hoffer JM (eds) Trans-Pecos region, southeastern New Mexico and west Texas. New Mexico Geol Soc 31st Field Conference, pp 173–178.

Klimchouk A., Andrejchuk V. (1996). Environmental Problems in Gypsum Karst Terrains. Int. J. Speleol. 25 (3-4) 145-156

Lagerwerff J.V., Akin G.W., Moses S.W. (1965). Detection and Determination of Gypsum in Soils. Proceedings of the Soil Science Society of America 29:535-540.

Montgomery C.W (2000). Environmental Geology 5th edition update pp 546

Morris J. (2018). Physical and Chemical controls on Suffosion Development in Gypsic Soils. MSc. Thesis. Stephen F. Austin State University, Nacogdoches, Texas.

Nelson R.E. (1982). Carbonate and Gypsum. In: Page, A.L. et al. Ed.., Methods of Soil Analysis, Part 2, 2nd edn. SSSA, Agronomy Monograph, Vol. 9. Madison, WI, pp. 181–197.

Porta J. (1998) Methodologies for the Analysis and Characterization of Gypsum Soils: A Review. Geoderma 87 (1998) 31-46.

Stafford K.W., Rosales-Lagarde L., Boston P.J. (2008a). Castile evaporite karst potential map of the Gypsum Plain, Eddy County, New Mexico and Culberson County, Texas: A GIS methodological comparison. Journal of Cave and Karst Studies 70 (1): 35-46.

Stafford K.W., Nance R., Rosales-Lagarde L., Boston P.J. (2008b). Epigene and Hypogene Karst Manifestations of the Castile Formation: Eddy County, New Mexico and Culberson County, Texas, USA. International Journal of Speleology 37 (2): 83-98.

Stafford K.W. (2013). Evaporite Karst and Hydrogeology of the Castile Formation: Culberson County, Texas and Eddy County, New Mexico Faculty Publications. 3. Retrieved from https://scholarworks.sfasu.edu/geology/3

Stafford K.W., Brown W.A. (2019). Initial Geohazard Potential Characterization of FM 2185

Texas Department of Transport. (2020). FM 2185 Proposed Improvements. Retrieved from https://www.txdot.gov/inside-txdot/projects/studies/el-paso/fm2185.html

Thierry P., Prunier-Laparmentier A., Lembezat C., Vanoudheusden E., Vernoux J. (2009) 3D Geological Modelling at Urban Scale and Mapping of Ground Movement Susceptibility from Gypsum Dissolution: The Paris Example (France). Engineering Geology. 105: 51-64.

Thompson A., Hine P., Peach D., Frost L., Brook D. (1998). Subsidence Hazard Assessment as a Basis for Planning Guidance in Ripon. In: Maund JG, Eddleston M (eds) Geohazards in engineering geology. Engineering Geology Spec Publ 15, Geological Society, London, pp 415–426

United Stated Department of Agriculture Handbook No.60 (1954). Diagnosis and Improvement of Saline and Alkaline Soils. Retrieved from https://www.ars.usda.gov/pacific-west-area/riverside-ca/agricultural-water-efficiency-and-salinity-research-unit/docs/publications/handbook-no-60/

United States Department of Agriculture, Natural Resources Conservation Service. (1997). Soil Climate Map, Soil Science Division, World Soil Resources, Washington D.C.

United States Department of Agriculture, Natural Resources Conservation Service. (2013). Soil Survey of Culberson County, Texas. Retrieved from http://soils.usda.gov/survey/printed_surveys/.

United States Department of Agriculture, Natural Resources Conservation Service (1999). Soil Survey Staff. Official Soil Series Descriptions. Available online.

United States Department of Agriculture, Natural Resources Conservation Service. (1999). Soil Taxonomy-A Basic System of Soil Classification for making and Interpreting Soil Surveys.

Verheye W. (2009). Soils of Arid and Semi-Arid Areas. Land Use, Land Cover and Soil Sciences. Encyclopedia of Life Support Systems (EOLSS) Vol. VII

Vieillefon J. (1979). Contribution to the Improvement of Analysis of Gypsiferous Soils. Cahiers/ORSTOM, Série Pédologie 17:195-223. Translated from Food and

Agriculture Organization of the United Nations. 1990. Management of Gypsiferous Soils. FAO Soils Bulletin 62. Rome

Weindorf D.C., Zhu Y., Ferrell R., Rolong N., Barnett T., Allen B.N., Herrero J. and Hudnall W. (2009). Evaluation of Portable X-ray Fluorescence for Gypsum Quantification in Soils. Soil Science 174 (10): 556-562 DOI:10.1097/SS.0b013e3181bbbd0b

Yaoru L., Cooper A.H. (1997). Gypsum Karst Geohazards in China. 117-126 in BECK, F.B. and STEPHENSON, J.B (Editors) The Engineering Geology and Hydrogeology of Karst Terranes. Proceedings of the Sixth Multidisciplinary Conference on Sinkholes and the Engineering and Environmental Impacts of Karst Springfield/Missouri/6-9 April 1997. A.A.Balkema, Rotterdam.

Yilmaz I. (2001). Gypsum/Anhydrite: Some Engineering Problems. Bull Eng Geol Env 59: 227-230

Yilmaz I. (2007). GIS based Susceptibility Mapping of Karst Depression in Gypsum: A Case Study from Sivas Basin (Turkey). Engineering Geology 90 (2007) 89-103. Elsevier B.V. DOI: 10.1016/j.enggeo.2006.12.004

Appendix 1: Gypsum concentration for the randomly selected samples tested using the wet chemical method.

	Sample No.	Water Extractable Sulfate(mg/kg)	Sulfur(mg/kg)	Sulfur from Sulfate(mg/kg)	Corrected Sulfur(mg/kg)	Gypsum(mg/kg)	Gypsum (g/kg)
Surface Samples	31	13,100.00	44,200.00	4,372.12	39,827.88	213,875.71	213.88
	179	12.50	932.00	4.17	927.83	4,982.44	4.98
	60	596.00	1,860.00	198.91	1,661.09	8,920.03	8.92
	87	7.77	1,210.00	2.59	1,207.41	6,483.77	6.48
	11	696.00	1,740.00	232.29	1,507.71	8,096.40	8.10
	119	4.64	2,720.00	1.55	2,718.45	14,598.08	14.60
	130	1,170.00	3,060.00	390.49	2,669.51	14,335.28	14.34
	79	64.20	1,580.00	21.43	1,558.57	8,369.54	8.37
	X	13,900.00	61,700.00	4,639.12	57,060.88	306,416.92	306.42
	189	16.80	1,230.00	5.61	1,224.39	6,574.99	6.57
Subsurface Samples	31	13,100.00	68,800.00	4,372.12	64,427.88	345,977.71	345.98
	179	5.97	882.00	1.99	880.01	4,725.64	4.73
	60	14,500.00	121,000.00	4,839.37	116,160.63	623,782.58	623.78
	87	8.45	1,410.00	2.82	1,407.18	7,556.56	7.56
	11	10,700.00	11,200.00	3,571.12	7,628.88	40,967.07	40.97
	119	15.80	2,530.00	5.27	2,524.73	13,557.78	13.56
	130	14,400.00	111,000.00	4,806.00	106,194.00	570,261.80	570.26
	79	21.30	1,470.00	7.11	1,462.89	7,855.73	7.86
	X	15,200.00	107,000.00	5,073.00	101,927.00	547,348.01	547.35
	189	15.10	1,130.00	5.04	1,124.96	6,041.04	6.04
Reagent-Grade Gypsum	A	16,400.00	175,000.00	5,473.50	169,526.50	910,357.33	910.36
	B	15,800.00	173,000.00	5,273.25	167,726.75	900,692.67	900.69

Appendix 2: Gypsum readings obtained from surface samples.

Sample No.	Coordinates		XRF readings			Thermogravimetry	
					Calculated	% Water	Calculated
	x	y	Sulfur(ppm)	Calcium(ppm)	Gypsum (%)	per 10g	Gypsum (%)
A	-104.2213	31.7530	12000.44	76961.86	5.9700	0.1318	6.3053
B	-104.2213	31.7566	9453.42	74903.84	5.4606	0.1768	8.4605
C	-104.2213	31.7602	265485.38	204269.48	56.6670	1.2813	61.3070
D	-104.2213	31.7639	278429.41	217645.73	59.2558	1.3768	65.8772
E	-104.2213	31.7675	5913.62	44501.79	4.7526	0.1089	5.2096
F	-104.2214	31.7711	138523.77	136569.50	31.2747	0.6755	32.3224
G	-104.2214	31.7748	3707.61	60969.16	4.3114	0.0759	3.6314
H	-104.2214	31.7784	3400.35	58013.50	4.2500	0.0569	2.7214
I	-104.2214	31.7820	3177.21	47110.17	4.2053	0.0440	2.1041
J	-104.2215	31.7856	101317.95	122058.91	23.8335	0.5489	26.2636
K	-104.2215	31.7893	4067.43	99178.84	4.3834	0.0558	2.6721
L	-104.2208	31.7928	7260.98	68707.39	5.0221	0.0637	3.0476
M	-104.2205	31.7964	4253.02	88270.58	4.4205	0.0478	2.2883
N	-104.2211	31.8000	4310.99	91471.41	4.4321	0.0621	2.9727
O	-104.2215	31.8036	3339.81	127581.84	4.2379	0.1101	5.2701
P	-104.2216	31.8072	32818.49	121681.94	10.1336	0.2467	11.8035
Q	-104.2216	31.8109	16405.13	100023.04	6.8509	0.1540	7.3689
R	-104.2207	31.8144	4663.39	123183.76	4.5026	0.0510	2.4417
S	-104.2204	31.8180	12583.69	104164.74	6.0866	0.1689	8.0811
T	-104.2205	31.8216	62332.52	107451.46	16.0364	0.3302	15.7985
U	-104.2207	31.8252	4493.94	140749.11	4.4687	0.0833	3.9865
V	-104.2208	31.8289	131902.41	133316.41	29.9504	0.4980	23.8281
W	-104.2209	31.8325	4904.15	85406.44	4.5507	0.0725	3.4672
X	-104.2212	31.8361	133486.39	133626.14	30.2672	0.6562	31.3962
Y	-104.2216	31.8397	190242.75	149818.55	41.6185	0.8071	38.6173
Z	-104.2217	31.8434	229336.92	199489.08	49.4373	0.9750	46.6510
AA	-104.2217	31.8470	184041.31	165955.16	40.3782	0.6825	32.6574
1	-104.2212	31.7494	18578.73	138796.56	7.2856	0.1727	8.2624
2	-104.2212	31.7458	123422.52	170564.34	28.2544	0.6703	32.0729
3	-104.2212	31.7422	2376.59	126085.52	4.0452	0.1036	4.9562
4	-104.2212	31.7386	49668.32	114416.30	13.5036	0.5286	25.2939
5	-104.2212	31.7349	7843.20	98691.55	5.1385	0.1336	6.3910
6	-104.2212	31.7313	3534.23	88141.46	4.2767	0.0818	3.9137

			Surface Samples				
Sample No.	Coordinates			XRF readings		Thermogravimetry	
					Calculated	% Water	Calculated
	x	y	Sulfur(ppm)	Calcium(ppm)	Gypsum (%)	per 10g	Gypsum (%)
7	-104.2218	31.7277	2149.20	71622.16	3.9997	0.0854	4.0847
8	-104.2229	31.7243	1451.57	80329.73	3.8602	0.0920	4.4015
9	-104.2219	31.7208	3370.55	97841.28	4.2440	0.0782	3.7419
10	-104.2211	31.7173	4369.18	83705.63	4.4437	0.1542	7.3771
11	-104.2211	31.7137	2267.70	101846.69	4.0234	0.0784	3.7490
12	-104.2210	31.7101	7139.33	102404.89	4.9978	0.1359	6.5029
13	-104.2210	31.7064	91158.76	155760.72	21.8017	0.7470	35.7402
14	-104.2210	31.7028	17819.98	142725.42	7.1339	0.1480	7.0826
15	-104.2210	31.6992	24955.72	115722.27	8.5610	0.2550	12.2003
16	-104.2209	31.6955	3038.20	87479.64	4.1775	0.0925	4.4269
17	-104.2209	31.6919	33243.37	124943.37	10.2186	0.2531	12.1090
18	-104.2209	31.6883	28928.08	125243.16	9.3555	0.2047	9.7922
19	-104.2208	31.6847	83061.59	166386.39	20.1822	0.7781	37.2311
20	-104.2208	31.6810	177719.28	200714.42	39.1138	1.2284	58.7746
21	-104.2207	31.6774	69219.27	145036.31	17.4138	0.6432	30.7765
22	-104.2207	31.6738	24136.92	96752.38	8.3973	0.1598	7.6474
23	-104.2206	31.6702	2791.66	79782.77	4.1282	0.1420	6.7959
24	-104.2206	31.6665	2720.48	70529.69	4.1140	0.1331	6.3693
25	-104.2220	31.6632	40712.80	105171.41	11.7125	0.2982	14.2685
26	-104.2240	31.6599	22360.53	134986.36	8.0420	0.2009	9.6101
27	-104.2258	31.6567	197528.34	205045.69	43.0756	1.4371	68.7604
28	-104.2277	31.6534	120008.52	160704.86	27.5716	0.7882	37.7106
30	-104.2302	31.6505	204420.13	165645.55	44.4539	1.3577	64.9598
31	-104.2329	31.6477	71073.52	130047.99	17.7846	0.6530	31.2447
32	-104.2366	31.6460	3736.68	68146.16	4.3172	0.2279	10.9058
33	-104.2404	31.6442	220773.47	202465.20	47.7246	1.5807	75.6339
34	-104.2440	31.6423	116099.85	133702.19	26.7899	0.7583	36.2829
35	-104.2471	31.6399	29694.21	78713.30	9.5087	0.2712	12.9773
36	-104.2502	31.6374	189669.72	178904.69	41.5038	1.0714	51.2645
37	-104.2524	31.6344	152531.13	151773.22	34.0761	0.7218	34.5358
38	-104.2550	31.6316	2821.40	42342.67	4.1342	0.1630	7.7970
39	-104.2584	31.6294	25463.86	74608.11	8.6627	0.3618	17.3092
40	-104.2618	31.6272	2401.33	48214.51	4.0502	0.1393	6.6654
41	-104.2644	31.6244	2965.09	51241.13	4.1629	0.1439	6.8869

	Surface Samples						
Sample No.	Coordinates			XRF readings		Thermogravimetry	
	x	y	Sulfur(ppm)	Calcium(ppm)	Calculated Gypsum (%)	% Water per 10g	Calculated Gypsum (%)
42	-104.2656	31.6209	2212.65	61209.66	4.0124	0.0712	3.4053
43	-104.2679	31.6179	2618.73	85869.57	4.0936	0.0648	3.1000
44	-104.2702	31.6148	2126.45	86539.16	3.9952	0.0715	3.4234
45	-104.2726	31.6118	3098.43	65267.41	4.1896	0.1217	5.8226
46	-104.2749	31.6088			3.5699	0.1229	5.8813
47	-104.2772	31.6057	278268.59	227658.09	59.2236	1.6029	76.6941
48	-104.2795	31.6027	116610.13	118797.59	26.8919	0.5037	24.1008
49	-104.2817	31.5996	2464.00	81062.80	4.0627	0.0883	4.2265
50	-104.2839	31.5965	235783.23	187723.92	50.7265	1.1278	53.9594
51	-104.2861	31.5934	146456.98	127973.73	32.8613	0.7217	34.5328
52	-104.2892	31.5909	2710.77	99087.70	4.1121	0.0895	4.2813
53	-104.2924	31.5887	81484.81	91114.11	19.8669	0.2940	14.0678
54	-104.2946	31.5856	3456.69	61781.04	4.2612	0.1543	7.3821
55	-104.2967	31.5825	1742.85	29855.33	3.9185	0.1526	7.3011
56	-104.2988	31.5793	166032.05	153867.53	36.7763	0.5431	25.9844
57	-104.3009	31.5762	3567.22	61098.84	4.2833	0.1139	5.4514
58	-104.3030	31.5731	15341.69	89236.52	6.6382	0.1383	6.6154
59	-104.3059	31.5705	1309.08	67768.96	3.8317	0.1484	7.1017
60	-104.3095	31.5686	7115.73	108021.59	4.9930	0.0862	4.1228
61	-104.3132	31.5669	968.72	67616.66	3.7636	0.0791	3.7851
62	-104.3169	31.5650	3963.63	61610.24	4.3626	0.0840	4.0169
63	-104.3205	31.5632	1977.39	57111.80	3.9654	0.1000	4.7863
64	-104.3242	31.5614	5897.12	54180.57	4.7493	0.1019	4.8739
65	-104.3278	31.5595	3929.85	100124.44	4.3559	0.0669	3.1986
66	-104.3314	31.5577	41518.51	72721.83	11.8736	0.2334	11.1678
67	-104.3351	31.5559	1515.31	44144.49	3.8730	0.1364	6.5270
68	-104.3388	31.5541	72051.36	93340.49	17.9802	0.3767	18.0247
69	-104.3424	31.5523	4634.63	57417.92	4.4968	0.1326	6.3465
70	-104.3461	31.5504	85657.07	91970.18	20.7013	0.4304	20.5911
71	-104.3499	31.5489	37853.20	72468.65	11.1405	0.2841	13.5919
72	-104.3539	31.5477	12632.19	80168.05	6.0963	0.1342	6.4230
73	-104.3579	31.5466	91966.20	104134.17	21.9631	0.4264	20.3998
74	-104.3619	31.5454	107057.42	90308.18	24.9814	0.4614	22.0762
75	-104.3659	31.5443	8358.42	57221.83	5.2416	0.1718	8.2195

	Surface Samples						
Sample No.	Coordinates			XRF readings		Thermogravimetry	
					Calculated	% Water	Calculated
	x	y	Sulfur(ppm)	Calcium(ppm)	Gypsum (%)	per 10g	Gypsum (%)
76	-104.3699	31.5431	221044.48	173757.36	47.7788	1.1617	55.5840
77	-104.3739	31.5419	32006.50	74660.27	9.9712	0.1815	8.6822
78	-104.3779	31.5408	29959.29	82511.78	9.5618	0.1529	7.3151
79	-104.3820	31.5396	11466.85	70976.62	5.8633	0.1538	7.3599
80	-104.3860	31.5385	24306.45	68136.88	8.4312	0.1749	8.3680
81	-104.3890	31.5361	217621.16	159951.83	47.0941	1.0712	51.2539
82	-104.3901	31.5326	12602.39	74193.63	6.0904	0.0731	3.4991
83	-104.3908	31.5290	18765.58	105660.96	7.3230	0.1026	4.9074
84	-104.3915	31.5254	9426.49	70201.00	5.4552	0.1041	4.9793
85	-104.3923	31.5219	9360.06	81304.63	5.4419	0.2147	10.2735
86	-104.3930	31.5183	12693.53	82725.77	6.1086	0.1113	5.3271
87	-104.3943	31.5149	7357.60	63289.30	5.0414	0.0756	3.6172
88	-104.3974	31.5124	8447.36	102864.70	5.2594	0.1014	4.8522
89	-104.4002	31.5097	9661.12	68843.70	5.5021	0.0924	4.4187
90	-104.4028	31.5068	10461.48	83025.27	5.6622	0.0745	3.5629
91	-104.4053	31.5039	13130.79	67099.45	6.1961	0.1195	5.7182
92	-104.4078	31.5010	7397.83	66025.09	5.0495	0.1139	5.4477
93	-104.4103	31.4981	1055.82	53908.39	3.7811	0.0795	3.8045
94	-104.4126	31.4951	1280.00	51100.13	3.8259	0.1071	5.1223
95	-104.4139	31.4916	1132.13	39186.90	3.7963	0.0769	3.6805
96	-104.4151	31.4881	974.07	57908.30	3.7647	0.0755	3.6136
97	-104.4167	31.4848	975.41	34956.91	3.7650	0.0495	2.3667
98	-104.4199	31.4824	1106.11	34997.83	3.7911	0.1019	4.8737
99	-104.4232	31.4801	1181.81	66779.70	3.8063	0.0454	2.1715
100	-104.4266	31.4780	858.16	37692.93	3.7415	0.0620	2.9654
101	-104.4303	31.4762	1359.67	54676.40	3.8418	0.0433	2.0729
102	-104.4338	31.4743	680.77	57099.32	3.7061	0.0411	1.9683
103	-104.4354	31.4710	1367.43	66242.54	3.8434	0.0709	3.3947
104	-104.4364	31.4674	1632.30	89236.47	3.8964	0.1319	6.3110
105	-104.4368	31.4639	856.38	59541.15	3.7412	0.0638	3.0508
106	-104.4361	31.4603	902.28	51165.71	3.7504	0.0748	3.5792
107	-104.4371	31.4569	735.58	33438.90	3.7170	0.0397	1.9012
108	-104.4392	31.4537	1209.48	40530.20	3.8118	0.0466	2.2289
109	-104.4414	31.4506	1952.75	42940.16	3.9605	0.0809	3.8713

				Surface Samples			
Sample No.	Coordinates			XRF readings		Thermogravimetry	
					Calculated	% Water	Calculated
	x	y	Sulfur(ppm)	Calcium(ppm)	Gypsum (%)	per 10g	Gypsum (%)
110	-104.4435	31.4475	1129.89	39746.18	3.7959	0.0805	3.8506
111	-104.4456	31.4443	2110.87	50830.89	3.9921	0.0764	3.6576
112	-104.4477	31.4412	2235.23	73958.94	4.0169	0.0583	2.7891
113	-104.4497	31.4380	2394.10	85520.63	4.0487	0.0606	2.9016
114	-104.4518	31.4348	2650.44	109662.87	4.1000	0.0712	3.4081
115	-104.4538	31.4316	2037.54	50728.46	3.9774	0.0390	1.8659
116	-104.4554	31.4283	1502.69	49047.31	3.8704	0.0513	2.4559
117	-104.4555	31.4247	1654.04	71246.12	3.9007	0.0456	2.1830
118	-104.4542	31.4212	2133.00	145489.72	3.9965	0.0417	1.9976
119	-104.4532	31.4177	1548.25	114129.21	3.8796	0.0501	2.3978
120	-104.4549	31.4144	1919.69	159381.44	3.9538	0.0486	2.3231
121	-104.4569	31.4112			3.5699		
122	-104.4587	31.4080	875.26	107558.34	3.7450	0.1305	6.2449
123	-104.4605	31.4047	12009.44	153268.06	5.9718	0.1901	9.0946
124	-104.4622	31.4014	749.21	117986.39	3.7197	0.0644	3.0817
125	-104.4635	31.3979	634.05	95161.48	3.6967	0.1438	6.8781
126	-104.4647	31.3944	977.73	176460.23	3.7654	0.0617	2.9510
127	-104.4663	31.3911	1433.20	87965.78	3.8565	0.0620	2.9667
128	-104.4692	31.3884	28223.45	113619.46	9.2146	0.2657	12.7122
129	-104.4712	31.3854	54094.94	116867.64	14.3889	0.3895	18.6369
130	-104.4711	31.3817	4311.17	158181.28	4.4321	0.0681	3.2571
131	-104.4709	31.3781	19089.01	105855.88	7.3877	0.2493	11.9281
132	-104.4706	31.3745	91472.21	127349.66	21.8643	0.6309	30.1878
133	-104.4704	31.3708	135191.42	162812.02	30.6082	0.9420	45.0723
134	-104.4702	31.3672	8794.97	113050.23	5.3289	0.1776	8.4998
135	-104.4700	31.3636	6385.59	109473.63	4.8470	0.1268	6.0682
136	-104.4698	31.3600	9446.78	107183.51	5.4593	0.1444	6.9080
137	-104.4696	31.3564	164714.42	193814.22	36.5128	1.2709	60.8079
138	-104.4709	31.3530	4325.47	84642.70	4.4350	0.1430	6.8443
139	-104.4741	31.3507	278010.44	232907.03	59.1720	1.8638	89.1754
140	-104.4774	31.3483	6899.11	169484.38	4.9497	0.0820	3.9219
141	-104.4806	31.3460	2000.43	123549.36	3.9700	0.1148	5.4919
142	-104.4838	31.3437	1096.15	54777.47	3.7891	0.1737	8.3088
143	-104.4870	31.3413	81791.73	144256.20	19.9282	0.6149	29.4199

	Surface Samples						
Sample No.	Coordinates			XRF readings		Thermogravimetry	
					Calculated	% Water	Calculated
	x	y	Sulfur(ppm)	Calcium(ppm)	Gypsum (%)	per 10g	Gypsum (%)
144	-104.4903	31.3390	32708.14	141773.69	10.1115	0.2614	12.5049
145	-104.4935	31.3366	1379.68	145094.73	3.8458	0.0737	3.5273
146	-104.4967	31.3343	1431.85	113836.26	3.8563	0.1500	7.1764
147	-104.4999	31.3319	1033.58	83098.76	3.7766	0.1696	8.1166
148	-104.5032	31.3296	964.05	114969.83	3.7627	0.0739	3.5375
149	-104.5066	31.3275	1008.11	82040.21	3.7715	0.0702	3.3589
150	-104.5104	31.3259	1049.59	57660.65	3.7798	0.1152	5.5120
151	-104.5138	31.3238	1060.01	67242.15	3.7819	0.1111	5.3144
152	-104.5171	31.3217	1069.04	73120.20	3.7837	0.0766	3.6643
153	-104.5209	31.3200	1330.75	76113.89	3.8361	0.0660	3.1561
154	-104.5245	31.3181	902.87	89660.95	3.7505	0.0686	3.2843
155	-104.5277	31.3157	1089.10	87575.68	3.7877	0.0987	4.7242
156	-104.5314	31.3142	1298.10	116815.93	3.8295	0.1075	5.1448
157	-104.5355	31.3133	103330.35	227171.81	24.2360	0.7661	36.6575
158	-104.5386	31.3109	1384.40	142697.98	3.8468	0.0721	3.4484
159	-104.5417	31.3084	1160.08	253255.73	3.8019	0.1144	5.4742
160	-104.5458	31.3079	1305.47	117327.05	3.8310	0.0738	3.5292
161	-104.5500	31.3076	1483.88	194786.67	3.8667	0.0544	2.6010
162	-104.5538	31.3060	1560.96	180328.91	3.8821	0.0871	4.1666
163	-104.5575	31.3042	1138.98	136081.27	3.7977	0.0523	2.5018
164	-104.5611	31.3024	981.42	105896.55	3.7662	0.0678	3.2433
165	-104.5648	31.3005	924.06	103252.13	3.7547	0.0642	3.0740
166	-104.5684	31.2987	1310.83	99009.49	3.8321	0.0620	2.9682
167	-104.5721	31.2969	1036.38	138910.13	3.7772	0.0845	4.0418
168	-104.5757	31.2950	1181.39	104144.88	3.8062	0.0658	3.1498
169	-104.5792	31.2930	897.84	96263.28	3.7495	0.0518	2.4791
170	-104.5813	31.2899	935.56	135664.80	3.7570	0.0744	3.5615
171	-104.5841	31.2872	903.75	53224.04	3.7507	0.0800	3.8265
172	-104.5866	31.2842	1028.36	57980.77	3.7756	0.0550	2.6338
173	-104.5889	31.2812	1122.54	72554.22	3.7944	0.0704	3.3663
174	-104.5913	31.2783	1149.59	99112.34	3.7998	0.0605	2.8969
175	-104.5937	31.2753	1110.01	65972.97	3.7919	0.0603	2.8864
176	-104.5961	31.2723	1054.86	97024.37	3.7809	0.0834	3.9918
177	-104.5985	31.2693	968.42	76190.56	3.7636	0.0543	2.5992

Sample No.	Coordinates		XRF readings			Thermogravimetry	
					Calculated	% Water	Calculated
	x	y	Sulfur(ppm)	Calcium(ppm)	Gypsum (%)	per 10g	Gypsum (%)
178	-104.6006	31.2662	994.96	87224.53	3.7689	0.0689	3.2949
179	-104.6014	31.2626	1064.56	81817.65	3.7828	0.0640	3.0612
180	-104.6019	31.2590	1092.64	74879.85	3.7884	0.0604	2.8897
181	-104.6025	31.2555	1100.42	84721.94	3.7900	0.0868	4.1551
182	-104.6030	31.2519	1048.40	75522.59	3.7796	0.0860	4.1129
183	-104.6043	31.2484	1399.61	119728.55	3.8498	0.1251	5.9835
184	-104.6053	31.2449	1130.98	93822.24	3.7961	0.0876	4.1922
185	-104.6051	31.2413	1067.82	75985.41	3.7835	0.0757	3.6236
186	-104.6049	31.2377	1047.39	87080.08	3.7794	0.0800	3.8265
187	-104.6042	31.2341	1212.49	106575.71	3.8124	0.1263	6.0408
188	-104.6034	31.2305	954.15	97396.81	3.7607	0.1238	5.9233
189	-104.6027	31.2269	911.21	83715.34	3.7521	0.1073	5.1331
190	-104.6019	31.2234	1100.68	94909.43	3.7900	0.0934	4.4681
191	-104.6012	31.2198	1028.55	86912.97	3.7756	0.1185	5.6696
192	-104.6004	31.2162	1210.60	75845.05	3.8120	0.1499	7.1732
193	-104.5997	31.2127	959.46	65010.45	3.7618	0.1183	5.6606
194	-104.5989	31.2091	1019.62	51700.64	3.7738	0.0574	2.7469
195	-104.5981	31.2056	700.37	65060.64	3.7100	0.0604	2.8922
196	-104.5974	31.2020	943.88	50003.74	3.7587	0.0619	2.9608
197	-104.5966	31.1984	951.19	47241.17	3.7601	0.0567	2.7118
198	-104.5959	31.1949	927.58	33463.20	3.7554	0.0573	2.7410
199	-104.5951	31.1913	1127.82	27050.83	3.7955	0.0467	2.2334
200	-104.5946	31.1877	1072.74	60167.13	3.7844	0.0842	4.0286
201	-104.5953	31.1841	776.51	31077.81	3.7252	0.0386	1.8489
202	-104.5959	31.1806	954.85	51986.60	3.7609	0.0460	2.2018
203	-104.5966	31.1770	836.98	27804.86	3.7373	0.0284	1.3606
204	-104.5972	31.1734	788.77	14951.91	3.7277	0.0336	1.6098
205	-104.5979	31.1698	796.04	21905.44	3.7291	0.0279	1.3332
206	-104.5985	31.1662	914.48	10292.94	3.7528	0.0263	1.2595
207	-104.5992	31.1627	827.81	5144.36	3.7355	0.0222	1.0630
208	-104.5998	31.1591	753.75	4865.00	3.7207	0.0218	1.0413
209	-104.6004	31.1555	839.96	13140.58	3.7379	0.0387	1.8518
210	-104.6005	31.1519	817.10	31020.57	3.7333	0.0391	1.8722
211	-104.6007	31.1483	893.72	29741.65	3.7486	0.0619	2.9599

Surface Samples							
Sample No.	Coordinates		XRF readings		Calculated	Thermogravimetry	
						% Water	Calculated
	x	y	Sulfur(ppm)	Calcium(ppm)	Gypsum (%)	per 10g	Gypsum (%)
212	-104.6009	31.1446	783.73	5047.36	3.7266	0.0248	1.1851
213	-104.6011	31.1410	787.46	13237.78	3.7274	0.0196	0.9359
214	-104.6013	31.1374	715.31	9832.17	3.7130	0.0349	1.6686
215	-104.6016	31.1338	808.46	13665.64	3.7316	0.0249	1.1900

Appendix 3: Gypsum readings obtained from subsurface samples.

				Subsurface Samples			
	Coordinates			XRF readings		Thermogravimetry	
				Calcium	Calculated	% Water	Calculated
Sample No.	x	y	Sulfur (ppm)	(ppm)	Gypsum (%)	per 10g	Gypsum (%)
A	-104.2213	31.7530	13274.81	76983.97	8.0996	1.7487	8.3670
B	-104.2213	31.7566	276093.88	228759.31	86.9454	14.9675	71.6147
C	-104.2213	31.7602	276810.97	220732.06	87.1605	14.2171	68.0246
D	-104.2213	31.7639	284241.84	233030.42	89.3898	14.6539	70.1143
E	-104.2213	31.7675	5334.88	78531.82	5.7177	1.2129	5.8033
F	-104.2214	31.7711	233717.36	196343.19	74.2324	13.5863	65.0062
G	-104.2214	31.7748	4744.05	73398.05	5.5404	1.0183	4.8724
H	-104.2214	31.7784	3952.55	72911.18	5.3030	0.8280	3.9619
I	-104.2214	31.7820	2427.18	64369.05	4.8454	0.8569	4.0999
J	-104.2215	31.7856	33467.35	76122.13	14.1574	2.5770	12.3299
K	-104.2215	31.7893	62334.23	144918.58	22.8175	3.2636	15.6155
L	-104.2208	31.7928	66796.89	119605.43	24.1563	2.9935	14.3230
M	-104.2205	31.7964	6938.1	83011.66	6.1986	0.5378	2.5730
N	-104.2211	31.8000	2876.14	100704.61	4.9800	0.6681	3.1965
O	-104.2215	31.8036	4325.42	117342.59	5.4148	0.9013	4.3124
P	-104.2216	31.8072	43436.99	125210.17	17.1483	2.4390	11.6700
Q	-104.2216	31.8109	4928.24	78770.04	5.5957	1.1017	5.2715
R	-104.2207	31.8144	33670.44	142597.05	14.2183	2.6827	12.8359
S	-104.2204	31.8180	8138.85	78550.78	6.5589	1.5310	7.3254
T	-104.2205	31.8216	266974.44	216304.34	84.2095	14.0367	67.1614
U	-104.2207	31.8252	13648.61	144308.63	8.2118	1.2228	5.8505
V	-104.2208	31.8289	297689.34	236545.73	93.4240	14.9062	71.3215
W	-104.2209	31.8325	5560.57	127962.33	5.7854	0.7696	3.6824
X	-104.2212	31.8361	242182.69	198934.5	76.7720	13.9701	66.8425
Y	-104.2216	31.8397	213714.94	165485.83	68.2317	9.0715	43.4042
Z	-104.2217	31.8434	198555.72	179624.13	63.6839	8.5207	40.7688
AA	-104.2217	31.8470	196619.69	160208.44	63.1031	8.0265	38.4045
1	-104.2212	31.7494	156993.3	166114.5	51.2152	12.4213	59.4320
2	-104.2212	31.7458	179459.22	198159.23	57.9550	13.7403	65.7432
3	-104.2212	31.7422	1363.23	86426.24	4.5262	1.7417	8.3334
4	-104.2212	31.7386	189636.48	179406.05	61.0081	15.4661	74.0007
5	-104.2212	31.7349	110255.12	141132	37.1937	5.0496	24.1606

Appendix 3: Gypsum readings obtained from subsurface samples.

			Subsurface Samples				
	Coordinates			XRF readings		Thermogravimetry	
				Calcium	Calculated	% Water	Calculated
Sample No.	x	y	Sulfur (ppm)	(ppm)	Gypsum (%)	per 10g	Gypsum (%)
6	-104.2212	31.7313	4156.99	74551.59	5.3643	1.0802	5.1683
7	-104.2218	31.7277	1467.72	73392.31	4.5575	0.6917	3.3094
8	-104.2229	31.7243	1524.97	103426.41	4.5747	1.0658	5.0997
9	-104.2219	31.7208	4458.22	114527.82	5.4547	0.9970	4.7704
10	-104.2211	31.7173	4843.86	85793.66	5.5704	1.8922	9.0537
11	-104.2211	31.7137	26011.43	147428.02	11.9206	1.7454	8.3514
12	-104.2210	31.7101	58692.95	116853.09	21.7251	3.8614	18.4758
13	-104.2210	31.7064	254183.81	223452.11	80.3723	17.8969	85.6309
14	-104.2210	31.7028	9421.62	177551.83	6.9437	1.1370	5.4401
15	-104.2210	31.6992			4.1172	2.2444	10.7387
16	-104.2209	31.6955	11469.72	92179.67	7.5581	1.3792	6.5990
17	-104.2209	31.6919	32920.31	113372.38	13.9933	2.6738	12.7933
18	-104.2209	31.6883	8231.11	86220.55	6.5865	1.4225	6.8062
19	-104.2208	31.6847	205998.7	209028.48	65.9168	15.4569	73.9563
20	-104.2208	31.6810	258476.59	224525.53	81.6602	17.3132	82.8384
21	-104.2207	31.6774	72297.66	160484.08	25.8065	7.3966	35.3902
22	-104.2207	31.6738	232375.86	216386.22	73.8300	15.9290	76.2155
23	-104.2206	31.6702	146947.75	179996.72	48.2015	7.6431	36.5698
24	-104.2206	31.6665	1986.07	81243.6	4.7130	1.6937	8.1040
25	-104.2220	31.6632	248150.42	224248.11	78.5623	18.6530	89.2490
26	-104.2240	31.6599	173347.34	203826.03	56.1214	11.9190	57.0288
27	-104.2258	31.6567	232975.97	217450.55	74.0100	17.8350	85.3350
28	-104.2277	31.6534	144193.5	169262.11	47.3753	11.0078	52.6688
30	-104.2302	31.6505	260318.55	222526.86	82.2128	19.3785	92.7203
31	-104.2329	31.6477	77175.36	140009.23	27.2698	8.4635	40.4952
32	-104.2366	31.6460	2866.29	72596.52	4.9771	2.9592	14.1588
33	-104.2404	31.6442	215014.28	204901.81	68.6215	14.9619	71.5880
34	-104.2440	31.6423	34437.39	92662.73	14.4484	3.2318	15.4633
35	-104.2471	31.6399	42212.07	78319.78	16.7808	4.1986	20.0890
36	-104.2502	31.6374	277278.41	233506.34	87.3007	18.5313	88.6667
37	-104.2524	31.6344	279907.56	232741.05	88.0895	18.9987	90.9027
38	-104.2550	31.6316	105145.27	155137.41	35.6608	10.5545	50.5001

Appendix 3: Gypsum readings obtained from subsurface samples.

				Subsurface Samples			
	Coordinates			XRF readings		Thermogravimetry	
				Calcium	Calculated	% Water	Calculated
Sample No.	x	y	Sulfur (ppm)	(ppm)	Gypsum (%)	per 10g	Gypsum (%)
39	-104.2584	31.6294	271539.97	229745.95	85.5792	19.0417	91.1084
40	-104.2618	31.6272	2455	52416.11	4.8537	1.8617	8.9079
41	-104.2644	31.6244	4103.02	66634.71	5.3481	1.3547	6.4817
42	-104.2656	31.6209	4498	70203.73	5.4666	0.8698	4.1617
43	-104.2679	31.6179	2115.48	118235.39	4.7518	0.9076	4.3425
44	-104.2702	31.6148	1834.59	109072.97	4.6676	0.9518	4.5541
45	-104.2726	31.6118	1732.65	64689.68	4.6370	1.4141	6.7659
46	-104.2749	31.6088	2474.92	83807.66	4.8597	1.2774	6.1122
47	-104.2772	31.6057	304062.44	241385.41	95.3359	17.1807	82.2042
48	-104.2795	31.6027	280526.88	222903.5	88.2753	12.9980	62.1913
49	-104.2817	31.5996	1588.22	72652.37	4.5937	0.8812	4.2161
50	-104.2839	31.5965	282383.47	228281.48	88.8322	16.0557	76.8217
51	-104.2861	31.5934	263410.25	243469.77	83.1403	14.2737	68.2951
52	-104.2892	31.5909	2722.08	102356.18	4.9338	0.6844	3.2746
53	-104.2924	31.5887	231676.81	198506.27	73.6202	12.2216	58.4763
54	-104.2946	31.5856	4892.31	76687.13	5.5849	1.8663	8.9296
55	-104.2967	31.5825	727	35250.94	4.3353	1.9453	9.3078
56	-104.2988	31.5793	271793.81	223026.47	85.6553	14.9853	71.7000
57	-104.3009	31.5762	4314.82	78507.5	5.4116	1.3912	6.6562
58	-104.3030	31.5731	232325.38	207376.66	73.8148	10.2316	48.9548
59	-104.3059	31.5705	3011.84	91002.48	5.0208	1.9719	9.4348
60	-104.3095	31.5686	225862.13	212438.78	71.8758	11.7597	56.2666
61	-104.3132	31.5669	21894.66	121750.52	10.6856	1.5611	7.4692
62	-104.3169	31.5650	5690.44	63802.36	5.8243	1.1442	5.4749
63	-104.3205	31.5632	971.06	78396.98	4.4085	1.1981	5.7325
64	-104.3242	31.5614	49814.44	74468.39	19.0615	2.9759	14.2389
65	-104.3278	31.5595	5663.02	172542.84	5.8161	0.8819	4.2197
66	-104.3314	31.5577	236639.23	197952.22	75.1090	12.5512	60.0535
67	-104.3351	31.5559	5034.84	38834	5.6277	1.2906	6.1751
68	-104.3388	31.5541	267754.06	219376.39	84.4434	14.4603	69.1882
69	-104.3424	31.5523	2279.51	68151.65	4.8011	1.6092	7.6996
70	-104.3461	31.5504	275052.97	215511.42	86.6331	12.8099	61.2913

Appendix 3: Gypsum readings obtained from subsurface samples.

				Subsurface Samples			
	Coordinates			XRF readings		Thermogravimetry	
				Calcium	Calculated	% Water	Calculated
Sample No.	x	y	Sulfur (ppm)	(ppm)	Gypsum (%)	per 10g	Gypsum (%)
71	-104.3499	31.5489	272146	223790.61	85.7610	15.5740	74.5166
72	-104.3539	31.5477	126115.96	154157.41	41.9520	6.1494	29.4232
73	-104.3579	31.5466	274551.75	211768.56	86.4827	16.3132	78.0534
74	-104.3619	31.5454	290362.22	227246.88	91.2259	16.1843	77.4370
75	-104.3659	31.5443	276395.38	231119.8	87.0358	15.9052	76.1013
76	-104.3699	31.5431	277565.88	226505.78	87.3870	15.4733	74.0348
77	-104.3739	31.5419	241126.47	197647.06	76.4551	13.9040	66.5265
78	-104.3779	31.5408	191155.72	194907.81	61.4639	10.0290	47.9858
79	-104.3820	31.5396	12420.9	67138.22	7.8435	1.4701	7.0339
80	-104.3860	31.5385	219792.81	188379.67	70.0550	11.4261	54.6703
81	-104.3890	31.5361	293590.38	229540.69	92.1943	16.5439	79.1573
82	-104.3901	31.5326	10963.78	87820.39	7.4063	0.8634	4.1313
83	-104.3908	31.5290	156099.7	154247.63	50.9471	5.9758	28.5921
84	-104.3915	31.5254	9682.8	68412.11	7.0220	1.1665	5.5814
85	-104.3923	31.5219	8465.25	84722.31	6.6568	2.0525	9.8207
86	-104.3930	31.5183	8756.37	64329.3	6.7441	0.9503	4.5471
87	-104.3943	31.5149	7941.04	102042.37	6.4995	1.0456	5.0031
88	-104.3974	31.5124	9389.37	101360.94	6.9340	0.7612	3.6423
89	-104.4002	31.5097	9588.35	80331.23	6.9937	0.7826	3.7447
90	-104.4028	31.5068	10041.23	89985.66	7.1296	0.9628	4.6065
91	-104.4053	31.5039	8514.07	67431.78	6.6714	1.3619	6.5161
92	-104.4078	31.5010	7453.5	81041.18	6.3533	1.0826	5.1799
93	-104.4103	31.4981	1164.36	65559.47	4.4665	1.0544	5.0451
94	-104.4126	31.4951	1421.71	34676.68	4.5437	0.9141	4.3738
95	-104.4139	31.4916	1101.25	30170.05	4.4476	0.8430	4.0333
96	-104.4151	31.4881	1004.58	82300.37	4.4186	1.0940	5.2342
97	-104.4167	31.4848	1000.09	39805.19	4.4172	0.6852	3.2786
98	-104.4199	31.4824	1218.96	47963.36	4.4829	1.1364	5.4371
99	-104.4232	31.4801	998.71	69317.16	4.4168	0.6067	2.9028
100	-104.4266	31.4780	952	36290	4.4028	0.7431	3.5557
101	-104.4303	31.4762	745.25	54183.75	4.3408	0.4745	2.2701
102	-104.4338	31.4743	1178.45	52767.51	4.4707	0.3623	1.7336

Appendix 3: Gypsum readings obtained from subsurface samples.

				Subsurface Samples			
	Coordinates			XRF readings		Thermogravimetry	
				Calcium	Calculated	% Water	Calculated
Sample No.	x	y	Sulfur (ppm)	(ppm)	Gypsum (%)	per 10g	Gypsum (%)
103	-104.4354	31.4710	635.62	56359	4.3079	0.7631	3.6511
104	-104.4364	31.4674	940.11	73493.68	4.3992	1.3195	6.3134
105	-104.4368	31.4639	965.59	56670.74	4.4069	0.5589	2.6740
106	-104.4361	31.4603	875.33	49998.89	4.3798	0.9124	4.3656
107	-104.4371	31.4569	1142.99	37417.46	4.4601	0.3784	1.8103
108	-104.4392	31.4537	1279.78	44418.71	4.5011	0.5433	2.5995
109	-104.4414	31.4506	679.46	47355.44	4.3210	0.8581	4.1059
110	-104.4435	31.4475	1134.62	35840.01	4.4576	0.8434	4.0353
111	-104.4456	31.4443	2430.36	54915.66	4.8463	0.7498	3.5874
112	-104.4477	31.4412	1928.85	64867.6	4.6959	0.5459	2.6121
113	-104.4497	31.4380	2215.87	113256.1	4.7820	0.5547	2.6541
114	-104.4518	31.4348	2305.4	141074.55	4.8088	0.8020	3.8375
115	-104.4538	31.4316	2408.26	40824.22	4.8397	0.4631	2.2158
116	-104.4554	31.4283	1673.51	44805.52	4.6193	0.6108	2.9226
117	-104.4555	31.4247	1257.79	68864.34	4.4945	0.4448	2.1280
118	-104.4542	31.4212	2765.35	118889.95	4.9468	0.5668	2.7120
119	-104.4532	31.4177	1927.59	131950.94	4.6955	0.8571	4.1012
120	-104.4549	31.4144	1459.29	151245.13	4.5550	0.7424	3.5520
121	-104.4569	31.4112	711.03	446510.53			
122	-104.4587	31.4080	1154.26	100487.69	4.4635	1.2770	6.1098
123	-104.4605	31.4047	238459.06	231480.16	75.6549	16.4369	78.6453
124	-104.4622	31.4014	1082.11	117647.56	4.4418	0.7916	3.7877
125	-104.4635	31.3979	772.89	99941.7	4.3491	1.6306	7.8020
126	-104.4647	31.3944	1102.1	144661.38	4.4478	1.0012	4.7904
127	-104.4663	31.3911	1190.6	135893.67	4.4744	0.7156	3.4237
128	-104.4692	31.3884	92480.3	154570.53	31.8613	10.9819	52.5452
129	-104.4712	31.3854	140140.91	163217.97	46.1595	9.2479	44.2484
130	-104.4711	31.3817	192007.66	214037.81	61.7195	13.4841	64.5171
131	-104.4709	31.3781	169541.36	182795.67	54.9796	12.9375	61.9019
132	-104.4706	31.3745	83102.16	128314.99	29.0478	4.5926	21.9743
133	-104.4704	31.3708	169495.67	180215.17	54.9659	12.3390	59.0383
134	-104.4702	31.3672	110661.88	170370.69	37.3158	8.5089	40.7124

Appendix 3: Gypsum readings obtained from subsurface samples.

						Thermogravimetry	
	Coordinates			XRF readings			
				Calcium	Calculated	% Water	Calculated
Sample No.	x	y	Sulfur (ppm)	(ppm)	Gypsum (%)	per 10g	Gypsum (%)
135	-104.4700	31.3636	158611.66	200422.25	51.7007	13.5668	64.9129
136	-104.4698	31.3600	89071.95	172799.03	30.8388	8.1307	38.9031
137	-104.4696	31.3564	260131.41	243092.63	82.1566	17.1691	82.1487
138	-104.4709	31.3530	8060.5	94706.25	6.5354	1.9962	9.5513
139	-104.4741	31.3507	286572.59	235124.5	90.0890	19.7118	94.3148
140	-104.4774	31.3483	137141.63	217195.73	45.2597	11.3357	54.2379
141	-104.4806	31.3460	74323.76	158891.52	26.4143	5.2503	25.1213
142	-104.4838	31.3437	12393.53	60079.35	7.8353	3.2061	15.3402
143	-104.4870	31.3413	177633.14	156011.63	57.4071	8.9762	42.9485
144	-104.4903	31.3390	111728.75	175742.16	37.6358	7.5805	36.2705
145	-104.4935	31.3366	1670.34	112984.43	4.6183	0.9639	4.6121
146	-104.4967	31.3343	1716.38	102901.45	4.6321	1.3131	6.2829
147	-104.4999	31.3319	1356.63	76914.31	4.5242	1.7247	8.2522
148	-104.5032	31.3296	1528.97	125957.69	4.5759	0.8826	4.2228
149	-104.5066	31.3275	1356.47	92718.02	4.5241	0.7628	3.6500
150	-104.5104	31.3259	2234.17	53384.32	4.7875	1.1240	5.3778
151	-104.5138	31.3238	2115.5	73793.39	4.7519	1.3075	6.2559
152	-104.5171	31.3217	1589.16	67835.58	4.5939	0.7090	3.3921
153	-104.5209	31.3200	1556.04	75617.48	4.5840	0.5516	2.6394
154	-104.5245	31.3181	2116.85	128986.88	4.7523	0.9113	4.3603
155	-104.5277	31.3157	1869.17	89695.73	4.6780	1.2090	5.7846
156	-104.5314	31.3142	2055.65	112407.64	4.7339	1.3598	6.5064
157	-104.5355	31.3133	115005.7	226203.41	38.6189	9.2451	44.2348
158	-104.5386	31.3109	1375.37	148760.34	4.5298	0.8658	4.1426
159	-104.5417	31.3084	1359.81	288493.19	4.5251	1.0948	5.2382
160	-104.5458	31.3079	2723.57	117491.4	4.9343	0.5692	2.7235
161	-104.5500	31.3076	1704.77	189377.55	4.6286	0.5859	2.8035
162	-104.5538	31.3060	1915.01	185962.3	4.6917	0.9395	4.4952
163	-104.5575	31.3042	1288.65	135837.52	4.5038	0.5001	2.3930
164	-104.5611	31.3024	1255.22	106254.29	4.4938	0.7012	3.3549
165	-104.5648	31.3005	1285.98	113063.74	4.5030	0.7579	3.6261
166	-104.5684	31.2987	1525.05	125219.23	4.5747	0.6814	3.2602

Appendix 3: Gypsum readings obtained from subsurface samples.

				Subsurface Samples			
	Coordinates			XRF readings		Thermogravimetry	
Sample No.	x	y	Sulfur (ppm)	Calcium (ppm)	Calculated Gypsum (%)	% Water per 10g	Calculated Gypsum (%)
167	-104.5721	31.2969	1783.64	146637.97	4.6523	0.9715	4.6483
168	-104.5757	31.2950	1285.79	113075.8	4.5029	0.8162	3.9051
169	-104.5792	31.2930	1234.57	140778.84	4.4876	0.5402	2.5846
170	-104.5813	31.2899	1640.13	167493.73	4.6092	0.7068	3.3820
171	-104.5841	31.2872	1136.35	71872.64	4.4581	0.9198	4.4009
172	-104.5866	31.2842	1300.86	77125.98	4.5075	0.7302	3.4939
173	-104.5889	31.2812	1272.72	98782.53	4.4990	0.7843	3.7527
174	-104.5913	31.2783	1352.78	141209.13	4.5230	0.7929	3.7938
175	-104.5937	31.2753	1011.31	83147.12	4.4206	0.6361	3.0437
176	-104.5961	31.2723	1637.54	96193.2	4.6085	0.7031	3.3642
177	-104.5985	31.2693	1512.64	98393.16	4.5710	0.6348	3.0373
178	-104.6006	31.2662	1468.93	121906.87	4.5579	0.6204	2.9685
179	-104.6014	31.2626	1366.08	82921.95	4.5270	0.6101	2.9194
180	-104.6019	31.2590	1334.11	77894.03	4.5174	0.7463	3.5707
181	-104.6025	31.2555	1396.12	89505.73	4.5360	0.9269	4.4351
182	-104.6030	31.2519	1402.83	89023.68	4.5380	1.0054	4.8106
183	-104.6043	31.2484	1377.85	113339.67	4.5306	1.0986	5.2562
184	-104.6053	31.2449	1474.38	113611.16	4.5595	1.0325	4.9402
185	-104.6051	31.2413	1148.41	85173.22	4.4617	1.0111	4.8379
186	-104.6049	31.2377	2523.69	101870.82	4.8743	0.8582	4.1064
187	-104.6042	31.2341	1739.75	90743.38	4.6391	1.1195	5.3565
188	-104.6034	31.2305	3157.16	93900.98	5.0643	1.4006	6.7012
189	-104.6027	31.2269	3646.73	97400.61	5.2112	1.0677	5.1087
190	-104.6019	31.2234	2417.01	135434.48	4.8423	1.2235	5.8541
191	-104.6012	31.2198	1917.33	89051.45	4.6924	1.2815	6.1315
192	-104.6004	31.2162	2711.53	85612.76	4.9307	1.5106	7.2276
193	-104.5997	31.2127	1969.79	69771.72	4.7081	1.1828	5.6591
194	-104.5989	31.2091	1986.57	67027.78	4.7132	0.6886	3.2947
195	-104.5981	31.2056	1900.47	48773.29	4.6873	0.5414	2.5904
196	-104.5974	31.2020	1513.26	49584.8	4.5712	0.4941	2.3643
197	-104.5966	31.1984	1433.46	41178.8	4.5472	0.6759	3.2339
198	-104.5959	31.1949	2081.21	38048.56	4.7416	0.6073	2.9060

Appendix 3: Gypsum readings obtained from subsurface samples.

		Subsurface Samples					
	Coordinates			XRF readings		Thermogravimetry	
Sample No.	x	y	Sulfur (ppm)	Calcium (ppm)	Calculated Gypsum (%)	% Water per 10g	Calculated Gypsum (%)
199	-104.5951	31.1913	1156.58	32696.64	4.4642	0.4783	2.2886
200	-104.5946	31.1877	1029.5	80809.86	4.4261	1.0361	4.9574
201	-104.5953	31.1841	922.99	40140.79	4.3941	0.3507	1.6780
202	-104.5959	31.1806	1165.18	62356.24	4.4668	0.3834	1.8344
203	-104.5966	31.1770	1064.32	34875.81	4.4365	0.2732	1.3073
204	-104.59722	31.1733961	858.6	14007.73	4.3748	0.3053	1.4610
205	-104.59787	31.1698154	1054.41	26167.37	4.4335	0.2986	1.4287
206	-104.59852	31.1662329	988.78	8290.07	4.4138	0.2674	1.2793
207	-104.59918	31.1626568	909.56	6506.34	4.3901	0.2244	1.0739
208	-104.59984	31.1590872	930.94	4660.59	4.3965	0.1831	0.8761
209	-104.60035	31.1554931	1184.58	10551.73	4.4726	0.2933	1.4035
210	-104.60055	31.1518773	1099.18	28047.94	4.4470	0.3586	1.7160
211	-104.60073	31.1482551	1072.49	22804.69	4.4389	0.5062	2.4222
212	-104.60092	31.1446311	886.84	6914.47	4.3833	0.2138	1.0229
213	-104.60111	31.1410087	1001.63	6109.36	4.4177	0.1842	0.8816
214	-104.6013	31.137383	960.64	9022.01	4.4054	0.2467	1.1804
215	-104.60162	31.1337657	1290.73	17135.5	4.5044	0.2415	1.1554

Appendix 4: Locations and average gypsum concentrations of clusters with high gypsum contents.

	From			To		Average Gypsum Concentration (%)			
Soil ID	Coordinates		Soil ID	Coordinates		Surface		Subsurface	
	x	y		x	y	Thermogravimetry	XRF	Thermogravimetry	XRF
W	-104.2209347	31.8325025	AA	-104.2217404	31.8470114	30.56	33.25	38.62	55.51
B	-104.2212782	31.7566260	E	-104.2213042	31.7675064	35.21	31.53	53.89	67.30
19	-104.2208090	31.6846658	22	-104.2206669	31.6737866	33.61	21.28	67.10	61.80
25	-104.2220430	31.6631647	40	-104.2617835	31.6271649	32.00	22.23	57.93	51.45
46	-104.2748741	31.6087533	52	-104.2891852	31.5909446	29.10	25.92	43.30	52.85
67	-104.3351118	31.5559070	77	-104.3739290	31.5419343	16.95	15.84	56.40	67.07
132	-104.4706485	31.3744731	136	-104.4702417	31.3672200	19.35	13.62	45.10	40.77
138	-104.4708953	31.3530185	140	-104.4773521	31.3483402	33.31	22.85	52.70	47.29

VITA

Chikaodili Ohakawa was born and raised in Lagos, Nigeria. Before attending Stephen F. Austin, she attended Nnamdi Azikiwe University Awka, Anambra state, Nigeria where she graduated with a Bachelor of Science in Geological Sciences. After graduating, Chika worked for about five years in Nigeria before moving to the United States and enrolling in the Graduate School of Stephen F. Austin State University to pursue a master's degree in environmental science in January 2019.

Permanent Address: 201 Lake Livingston Drive,

                       Georgetown, Texas 78628.

This thesis was typed by Chikaodili Ohakawa and is based on the APA style manual.